NBS

The Performance of A Conventional Residential Sized Heat Pump Operating With A Nonazeotropic Binary Refrigerant Mixture

William Mulroy
David Didion

U.S. DEPARTMENT OF COMMERCE
National Bureau of Standards
National Engineering Laboratory
Center for Building Technology
Building Equipment Division
Gaithersburg, MD 20899

October 1986

Sponsored By:
Office of Buildings and Community Systems
U.S. Department of Energy through
Oak Ridge National Laboratory under
Contract DE-AC05-84OR21400 with
Martin Marietta Energy Systems, Inc.

NBSIR 86-3422

THE PERFORMANCE OF A CONVENTIONAL RESIDENTIAL SIZED HEAT PUMP OPERATING WITH A NONAZEOTROPIC BINARY REFRIGERANT MIXTURE

William Mulroy
David Didion

U.S. DEPARTMENT OF COMMERCE
National Bureau of Standards
National Engineering Laboratory
Center for Building Technology
Building Equipment Division
Gaithersburg, MD 20899

October 1986

Sponsored By:
Office of Buildings and Community Systems
U.S. Department of Energy through
Oak Ridge National Laboratory under
contract DE-AC05-84OR21400 with
Martin Marietta Energy Systems, Inc.

U.S. DEPARTMENT OF COMMERCE, Malcolm Baldrige, *Secretary*
NATIONAL BUREAU OF STANDARDS, Ernest Ambler, *Director*

Executive Summary

As part of the Department of Energy (DoE)/Oak Ridge National Laboratory (ORNL) Building Equipment Research (BER) program, the National Bureau of Standards (NBS) performed laboratory tests of a relatively unmodified residential heat pump designed for R22 when charged with a nonazeotropic refrigerant mixture (NARM). Performance of the heat pump charged with a binary NARM of 65% R13B1/35% R152a was compared to R22. The advantages claimed for NARMs in this application are improved thermodynamic efficiency as a result of gliding refrigerant temperatures in the evaporator and condenser, and capacity modulation through composition shifting.

Four test series (at the DoE rating conditions) were conducted: 1) heat pump unmodified, 2) charge and expansion device area optimization tests, 3) tests to evaluate potential performance with wide shifts in NARM composition, and 4) tests with a receiver added to evaluate its ability to increase the NARM composition shift.

Efficiency improvement from the gliding temperature effect was found to be unlikely in an air-to-air heat pump or air conditioner because of the cross flow design of most current heat exchangers and, for heat pumps, because of the refrigerant flow reversal when switching from cooling mode to heating mode operation. The gliding temperature effect can; however, be successfully used in water-to-water applications.

The expansion device size should be changed when the refrigerant is changed for one of different properties (liquid versus vapor density); so as to ensure that proper subcooling will be maintained.

Capacity modulation through composition shift is a successful control strategy that will increase seasonal performance in northern applications.

It was shown that if a control strategy was used which maintained subcooling and composition could be shifted to 86% R13B1, heating capacity at 17°F could be increased 18% above that with R22 at comparable conditions.

Substitution of this particular NARM in the unmodified (except for expansion device optimization) heat pump resulted in improved low temperature (17°F) heating performance (up 6% in capacity, no change in efficiency) at the expense of reduced high-temperature heating (down 3% in efficiency) and cooling (down 12% in capacity, 11% in efficiency) performance.

Adding a receiver resulted in a greater composition shift at low air temperature and greater capacity enhancement relative to R22 (14% capacity increase, 2% efficiency increase).

No potential reliability or safety problems as a result of substitution of the NARM for R22 were observed.

It is recommended that future work on residential air conditioner and heat pump applications of NARM's be directed toward equipment redesign to better use their characteristics and to analysis of the performance characteristics and potential of other NARM's than the one tested for this report.

ABSTRACT

This report presents laboratory performance measurements of a relatively unmodified residential heat pump designed for R22 when charged with a nonazeotropic, binary mixture of R13B1 and R152a. Results are presented for various sizes of fixed expansion devices. The effect of gliding temperature within the saturation zone was found to be small. This experimental investigation confirmed that flash distillation within the accumulator would improve low temperature heating performance. The measured performance was approximately 11% lower in both efficiency and capacity than R22 for air conditioning. The high temperature heating efficiency was 3% lower than R22. The low temperature heating capacity was 14% higher and efficiency 2% higher than R22. These results show a substantial improvement over R22 for heating applications at the expense of reduced cooling mode performance. Further performance enhancement for this or other mixtures is expected through various system modifications which remain to be studied.

Key Words: air conditioning; heat pumps; non-azeotropic refrigerants; refrigerant mixtures; refrigerants; refrigeration.

TABLE OF CONTENTS

LIST OF FIGURES

LIST OF TABLES

SI CONVERSION FACTORS

MULTIPLY	BY	TO OBTAIN
Btu/h, Btuh	0.293	W
Btu/lbm°F, [C_p, specific heat]	4.19	kJ/kg°C
°F	°C = (°F - 32)/1.8	
ft	0.3048	m
ft/min, fpm	0.00508	m/s
ft^3/lbm	0.0623	m^3/kg
ft^3/min, CFM	0.472	m^3/s
gpm (US)	0.0631	L/S
inch	25.4	mm
inch of water	3.38	kPa
kBtu/h	0.2931	kW
lbm/h	0.000126	kg/s
ton of refrigeration capacity	3516	W

1. INTRODUCTION

The original goal of this study was to determine experimentally the energy performance benefits of a nonazeotropic binary refrigerant mixture in an unmodified residential heat pump. The single component refrigerant, R22, for which the unit tested was originally designed, was selected as a comparison basis. The mixture used in this study, R13B1/R152a, was chosen because it was one of several touted in the literature [1,2,3] as having potential for improving performance, and also because it was readily available from the manufacturer. This mixture may be considered as an example of any of a number of mixture possibilities and the quantitative values of this study are significant in that they indicate the relative merits of the different characteristics a mixture may offer (i.e., variable temperature phase change, variable capacity, bilevel temperature condensation/evaporation, etc.). Other mixtures may offer greater or lesser quantitative values depending on their properties. The determination of the optimum mixture for heat pumps was not a subject of this study.

As this study progressed it became apparent that a simple substitution of a refrigerant mixture for R22 was not a fair evaluation of the relative benefits of the mixture. The machinery components (i.e., heat exchangers, expansion device, compressor, etc.) had been originally sized for a particular refrigerant. The substitution of another refrigerant would cause the same machinery to perform differently not only because of thermodynamic properties differences, but also because parts of the machinery had become over- or undersized. Therefore the second part of this study focused on charge optimization and expansion device size determination.

A third series of tests was performed to evaluate the potential performance with greater composition shift than had been observed in previous tests.

A fourth series of tests was performed with a receiver added to evaluate the ability of this hardware addition to increase composition shift.

The heat pump performance criteria of prime consideration are capacity and efficiency. Of the two, capacity is often the more important because, for many applications (i.e., northern climates), an increased capacity at lower temperatures will reduce the resistance backup heat demand and thus significantly improve the seasonal efficiency. Performance criteria relating to reliability are also important and thus discharge pressure and temperature, suction pressure, pressure ratio, and pressure difference were measured and reported as well.

2. BACKGROUND

Nonazeotropic mixtures are those which exhibit a temperature change at constant pressure as they condense or evaporate. Binary mixtures consist of two components. This report deals exclusively with a binary nonazeotropic mixture of refrigerants R13B1 and R152a applied to a residential heat pump.

Several advantages have been claimed for nonazeotropic mixtures in refrigeration systems. Among these are improved thermodynamic efficiency (as a result of gliding temperatures in the two-phase zone, i.e. Lorenz vs. Carnot cycle) [4], multi-temperature level evaporators or condensers (useful for frozen and produce compartments in refrigerators and for domestic hot water in heat pumps and air conditioners) [5], and refrigerant composition change which alters the working media's capacity allowing it to match load requirements [6]. The last of these is the principal concern of this study.

The refrigerant mixture used in this study is one that has been recommended for heat pump applications [1,2,3]. In comparison to refrigerant 22, refrigerant 13B1 is more volatile, operating at higher pressures for equivalent saturation temperatures. It produces more capacity in a typical refrigeration system as a result of having a vapor density great enough to more than compensate for a smaller latent enthalpy change. However in a typical cycle [7], it is less efficient. Refrigerant 152a, in comparison, is of lower volatility, has a lower operating pressure, and is a lower capacity (lower vapor density) refrigerant with a relatively large latent enthalpy and high efficiency at higher evaporator temperatures. The mixture of the two, 65 percent by weight of R13B1, was chosen by DuPont to give capacity and efficiency similar to R22 during air conditioning operation and higher

capacity than R22 for heating operation after composition shift had taken place.

The greater the volatility difference between the two refrigerants, the easier it is to shift the composition of the circulating refrigerant from its initial value to one with a higher concentration of the higher boiling point component. This shifting may be effected passively by flash distillation in a conventional accumulator or actively with an added distillation system. The shifting process for the simple heat pump described within this report was a result of liquid flooding into the suction line accumulator during low ambient temperature of the heating mode only. This caused an increase of R13B1 in the composition of the circulating fluid.

When evaporation or condensation of a nonazeotrope takes place, the concentrations of the two components is different in the vapor and liquid phases. In particular, the vapor is always richer in the more volatile component and the liquid is always richer in the less volatile component in comparison to the initial composition. The extreme composition differences for this initial composition occur at the beginning and end of the phase change process. For example, as shown in figure 1, when a liquid mixture of 65% 13B1/35% 152a ($x_{\ell,a}$ in figure 1) at 90 psia, first reaches its bubble temperature, it will be in equilibrium with vapor at an approximate composition of 82% 13B1/18% 152a ($x_{v,a}$). An intermediate point approximately half way through the two phase region is shown in figure 1 at b to result in equilibrium between liquid 50% 13B1/50% 152a ($x_{\ell,b}$) and vapor 74% 13B1/26% 152a ($x_{v,b}$). The final example of

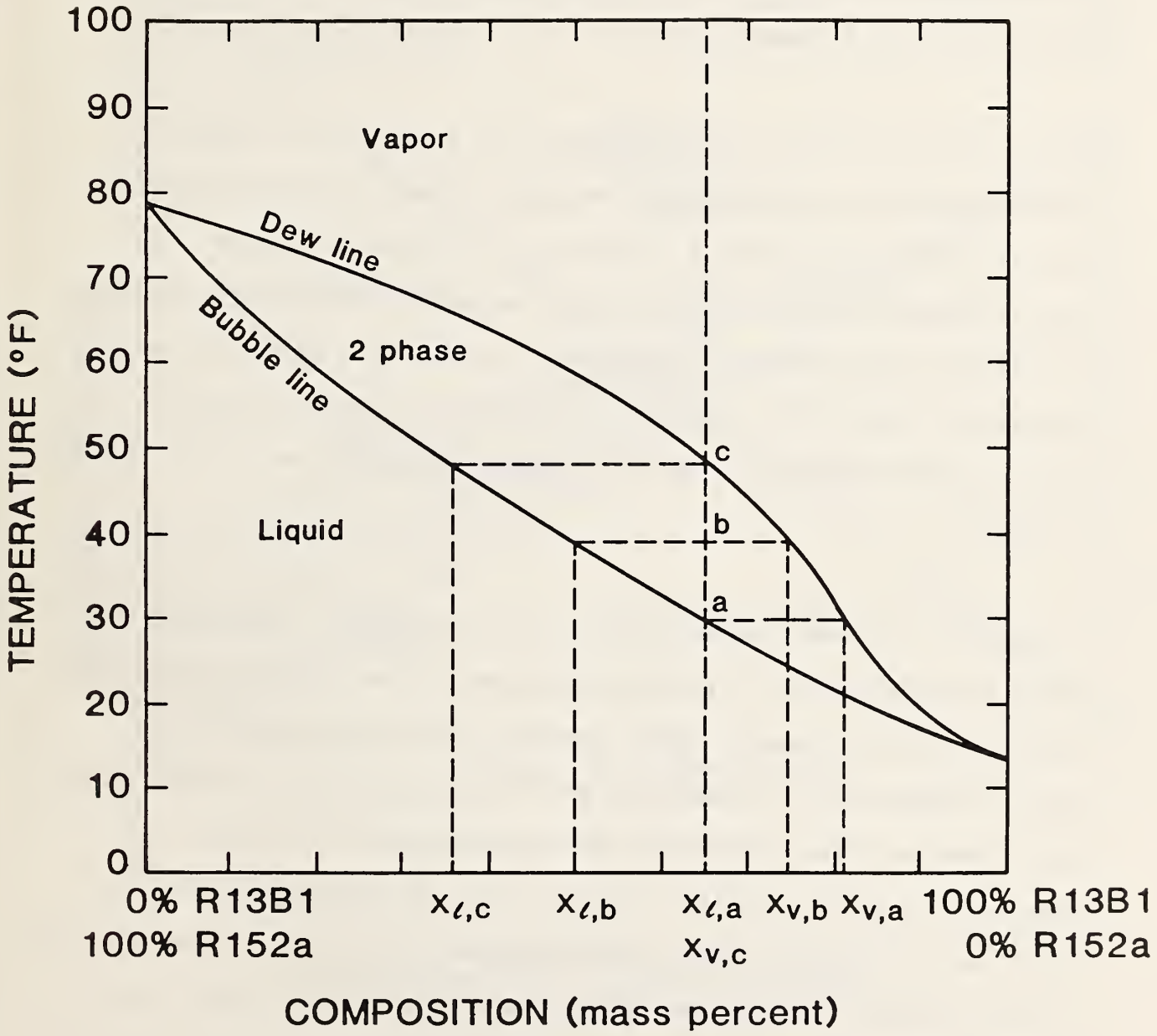

Figure 1. Dew and bubble temperatures for mixtures of R13B1 and R152a at a pressure of 90 psia.

figure 1 shows nearly completed evaporation at the dew line, c, where a liquid of 36% 13B1/64% 152a ($x_{\ell,c}$) is in equilibrium with vapor at the original 65% 13B1/35% 152a ($x_{v,c}$) composition.

Thus, refrigerant liquid in an accumulator will be quite rich in the less volatile component resulting in the remaining refrigerant being enriched in the more volatile refrigerant. In the case of the mixture used in these tests, flooding into the accumulator would increase the percentage of R13B1 circulating in the system and consequently increase low temperature heating capacity over that of R22 resulting in a substantial system efficiency increase by the reduction of need for electric resistance heat. This is shown in figure 2.

In addition to mixture characteristics, it is also useful to understand the system characteristics of a fixed expansion device heat pump that bring about flooding into the accumulator with consequent flash distillation at low outdoor temperatures. To understand this, two simplifications should be made. First, that mass flow through the fixed expansion device is choked, which is normally the case [8], and that, therefore, the expansion device mass flow will be only a function of high side refrigerant properties. Second, that the mass flow through the compressor is primarily a function of suction vapor density, that is the low side refrigerant properties.

In the heating mode, when the outdoor temperature decreases, the mass flow rate that the compressor pumps decreases because the suction vapor density decreases. The amount of liquid refrigerant that the expansion device can pass does not change because the indoor air temperature does not change and

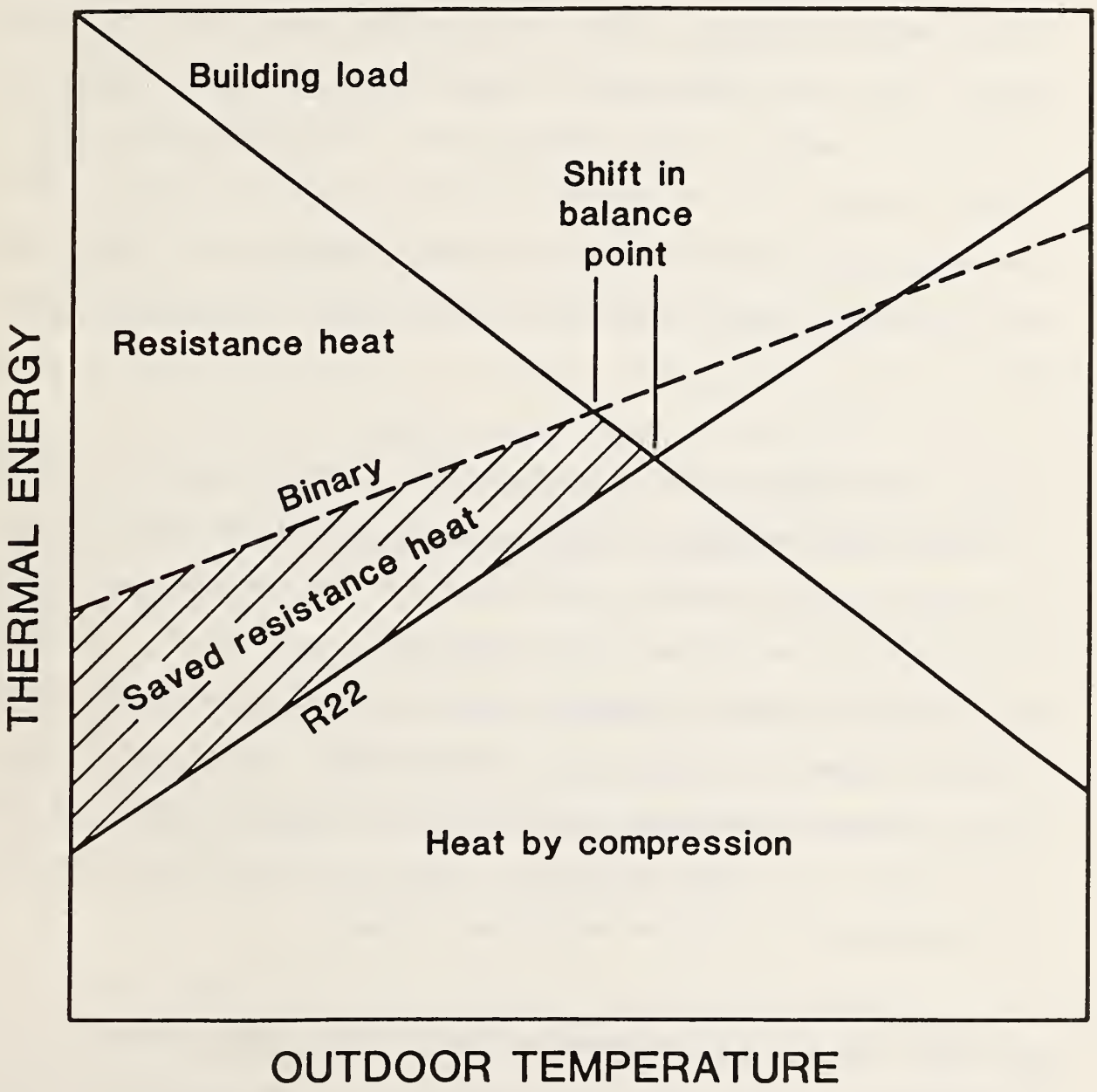

Figure 2. Energy savings as a result of increased low temperature compression system capacity reducing the need for "make-up" resistance heat.

hence the high side saturation state does not change significantly. When the outdoor temperature drops to such a level that the liquid mass flow that the expansion device can pass exceeds the vapor mass flow which the compressor is capable of pumping , liquid refrigerant will leave the condenser at a greater rate than it is replenished until subcooling is lost and two phase instead of liquid flow is passing through the expansion device. When steady state is reached, this two phase flow will be equal to the compressor mass flow.

In the cooling mode, as the outdoor temperature rises, the amount of liquid refrigerant that the expansion device can pass increases as a result of the increased saturation pressure in the condenser. The compressor capacity stays about the same since the indoor air temperature does not change. As before, expansion device capacity exceeding compressor capacity results ultimately in flooding through the evaporator into the accumulator. Conversely, if the outdoor temperature decreases, compressor capacity exceeding expansion device capacity will cause liquid refrigerant to back up in the condenser and cause the accumulator to be dry and subcooling to exist.

In either case the cycle accommodates itself to the changed outdoor temperature to achieve steady state with the mass flow through the compressor and expansion device equal. In the case of an expansion device capacity less than the compressor capacity, this is accomplished by a decrease in suction pressure and increase in head pressure that slightly increases expansion device flow and, as a result of this increased pressure difference, reduces the cycle efficiency. In the case of an overly large expansion device

compared to compressor capacity, the mass flow through the expansion device will be reduced to match the compressor capacity by passing vapor (which contributes little to capacity) as well as liquid refrigerant. This also reduces cycle efficiency.

In the control strategy for this binary mixture, it is not desired to have concentration shift at high temperature cooling even though this would help match the load line because it would result in high head pressures and reduced efficiency which would be undesirable for summer peaking utility applications. Hence the cooling expansion device orifice should be chosen to give enough superheat at the 82°F rating point to prevent flooding at higher outdoor ambient temperatures.

In heating the expansion device orifice should most likely be chosen to give best efficiency (i.e., a small amount of subcooling) at 47°F and to accept whatever degree of composition shift occurs at lower temperatures, although these criteria are less clear than those for cooling.

It should be noted that flooding into the accumulator is dependent on loss of subcooling in the condenser. More refrigerant in the accumulator means higher quality and void fraction in the condenser. Adding a receiver to the system as discussed for the last series of tests in this report increases system design flexibility by allowing varying (but equal in sum) amounts of refrigerant to be in the receiver and accumulator while maintaining a constant high side quality defined by the requirement that the receiver be at saturation conditions if it is partially full.

3. TEST HEAT PUMP AND FACILITY

A nominal three ton, split system, air-to-air unitary heat pump was used for this investigation. The outdoor unit contained the compressor, outdoor coil, fan defrost controller and associated equipment. The indoor and outdoor sections of the heat pump were installed in separate adjoining environmental chambers. The unit was tested in the environmental chambers and apparatus described in Reference [9].

The indoor section of the unit attached to the air flow measurement tunnel is shown in figure 3. The outdoor section of the unit with the cover removed to show the coil return bends is shown in figure 4.

The principal method used to measure the heat pump heating and sensible cooling capacities was the indoor air enthalpy method [10]. An air flowrate measuring apparatus was connected to an insulated duct attached to the discharge side of the indoor section of the heat pump. This apparatus consisted of a receiving chamber and discharge chamber separated by a partition containing a nozzle. An exhaust fan was attached to the duct leaving the discharge chamber so that the static pressure of the air leaving the indoor section of the heat pump could be adjusted to give air flow rates consistent with the manufacturer's performance data.

Manometers accurate to within 1% of the reading were used to measure the static pressure across the nozzle and pressures obtained by a pitot tube placed at the nozzle exit. A thermocouple was installed to determine the air temperature at the nozzle exit.

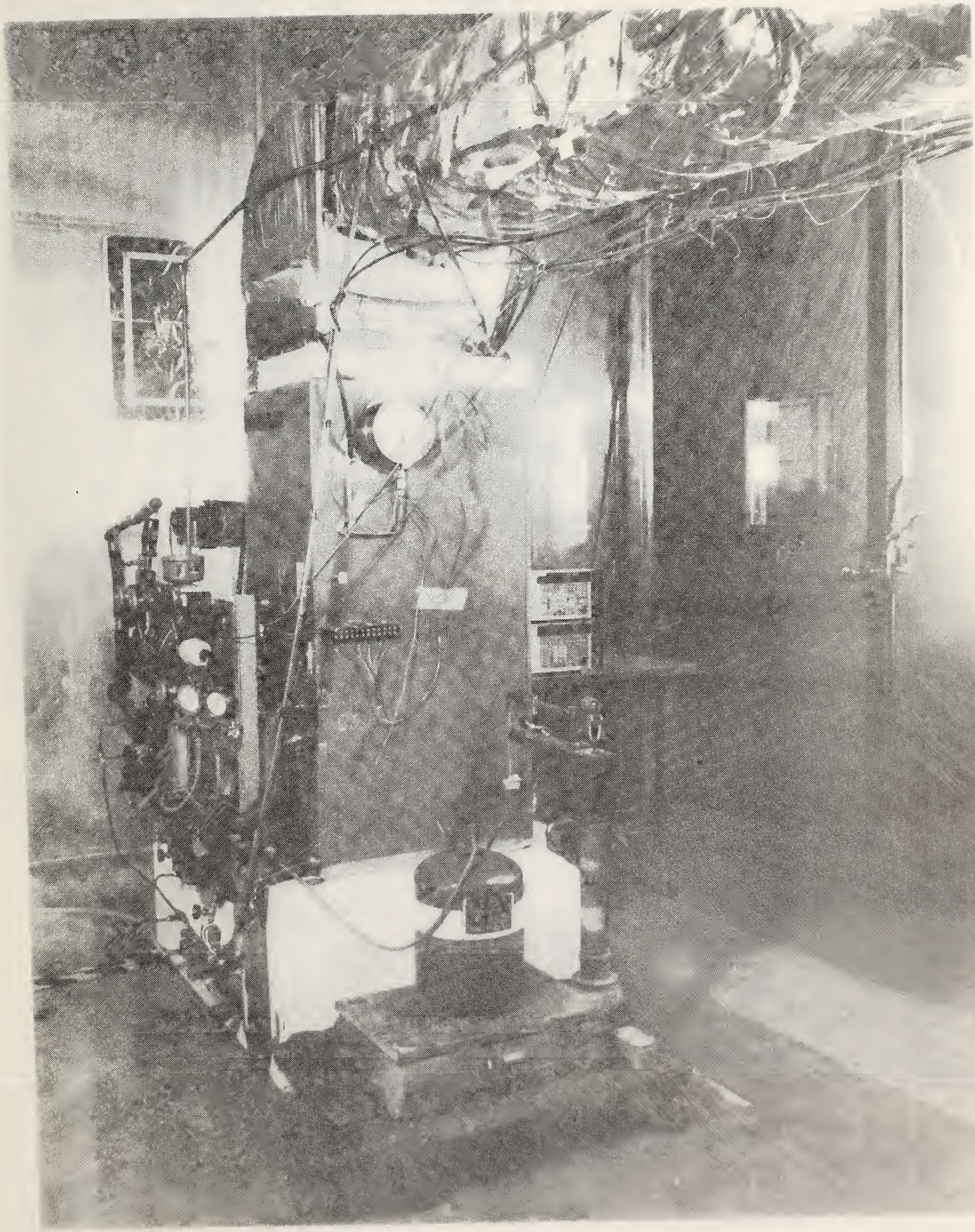

Figure 3. Heat pump indoor unit installed in test apparatus.

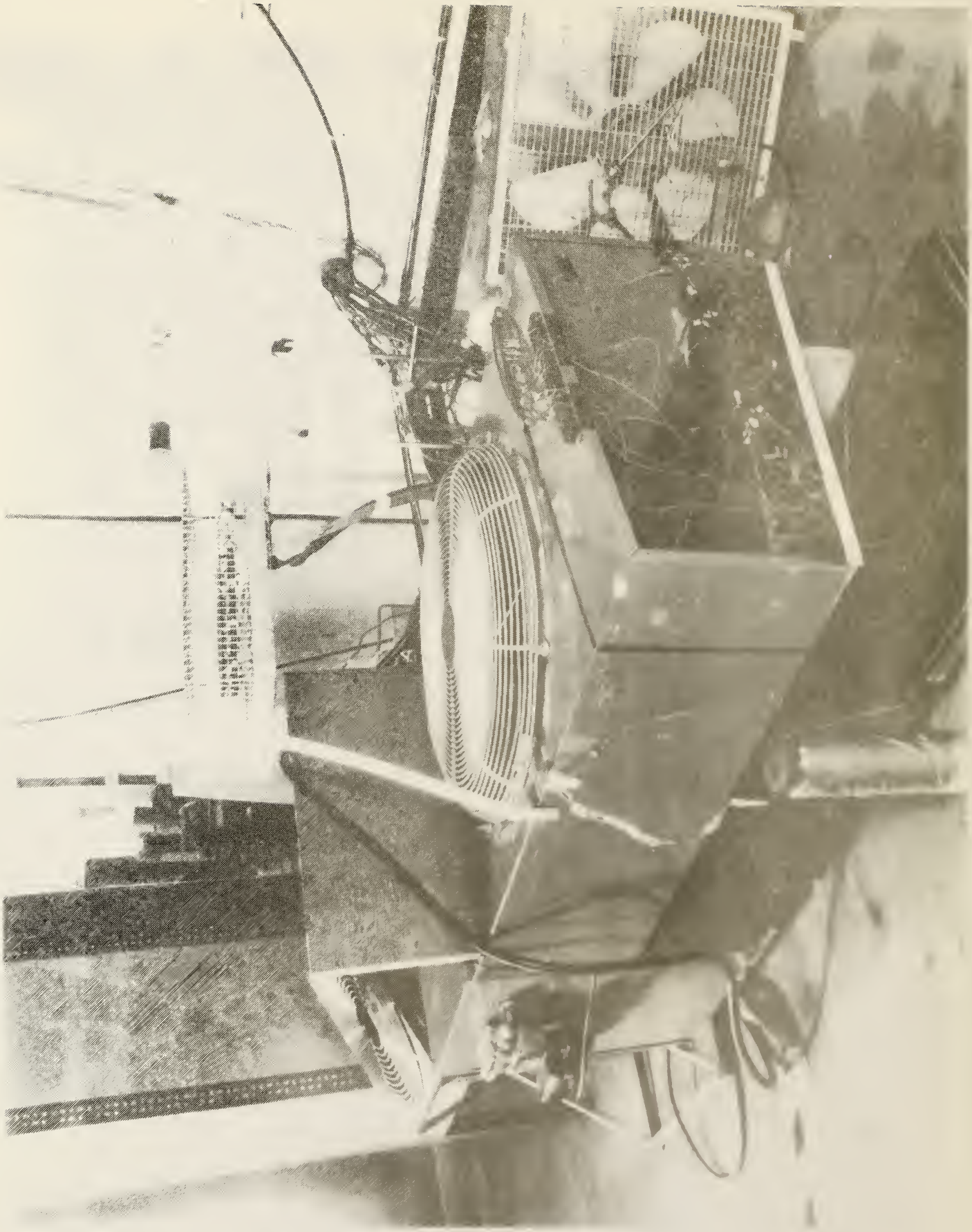

Figure 4. Heat pump outdoor unit.

A thirty-junction thermopile was used to measure the air temperature difference entering and leaving the indoor section of the heat pump. One side of the thermopile was placed in the entering duct while the other was placed in the insulated discharge duct leading to the receiving chamber of the air flow measuring apparatus. The junctions of the thermopile were spaced at centers of equal area across the inlet and discharge ducts.

The relative humidity of the air entering and leaving the indoor unit was measured using an aspirated psychrometer. An aspirated psychrometer was also used to measure the relative humidity of the air leaving the indoor unit during cooling mode tests and the relative humidity of the air entering the outdoor unit during heating mode tests.

The volatile refrigerant flow method [10] was used as the secondary test method. The liquid refrigerant line at the indoor unit was modified to incorporate a sightglass, turbine meter and four valves. The valves served to properly direct the flow of refrigerant through the turbine meter when the heat pump operated in either the heating or cooling mode. Adequate subcooling to prevent flashing at the turbine meter was necessary for accurate determination of the refrigerant flow rate. For this reason, it was not possible to use this secondary method for some tests. The refrigerant flow was determined by the turbine meter and an electronic totalizer. The density of the refrigerant was determined from the temperature and pressure readings and the mixture equations of state [11, 12].

Watthour meters were installed to measure the electrical energy consumption of the compressor and outdoor fan, and the indoor fan. Electronic totalizers

and printers were connected to the watt-hour meters to provide a record of the energy consumption.

The dry-bulb and dew-point temperatures in both the indoor and outdoor environmental chambers were continuously recorded. The average temperatures of the air entering the outdoor unit was measured using four thermocouples connected in parallel. In addition to the preceding instrumentation, thermocouples and pressure gauges were installed at various locations and temperatures and pressures were recorded to provide additional information on the performance of the unit and as a check for consistent operation.

At the conclusion of the initial test series the unit was modified by the addition of valved circuits in parallel with the capillary tubes to allow use of interchangeable orifices to facilitate expansion device optimization. A single orifice with a tee was used to replace the two capillary tubes on the indoor "A" coil. A manifold allowing selection between three orifices was used in place of the single capillary tube on the outdoor unit.

At this same time additional thermocouples were added to measure coil temperatures. Individual insulated thermocouples were soldered to all the return bends on one end of the outdoor coil and on one end of one half of the indoor coil.

Through-the-wall thermocouples were also installed through 13 return bends on the indoor coil and 9 return bends on the outdoor coil. In their most successful form these were created by silver-soldering an 18 gage hypodermic needle into a small hole drilled through the tube wall, inserting a

thermocouple, filling the base of the hypodermic with epoxy glue, evacuating the system sufficiently to draw the epoxy into the hypodermic needle, and finally crimping the back of the hypodermic needle. These through-the-wall thermocouples gave trouble throughout the project with leakage, particularly in the coil which happened to be operating as a condenser. For this reason, several of them were eliminated toward the end of the project.

Refrigerant composition for the binary-mixture tests was measured by withdrawing a small sample into a separate sample bottle which was later analyzed with a gas chromatograph.

A receiver installed in the liquid line near the indoor unit was used in some tests. An inverted oil separator with the oil return line blocked was used for this purpose. The internal volume of this oil separator shell used as a receiver was 140 cubic inches.

4. COOLING MODE TESTS

Cooling mode test results are summarized in Table 1 for tests performed using the binary refrigerant mixture and in Table 2 for tests performed using R22. As indicated, these tests were performed at either the DoE Test "A" (95°F outdoor ambient) or at the DoE Test "B" (82°F outdoor ambient) rating condition [13]. In both cases, the specified indoor entering condition is 80°F dry bulb and 67°F wet bulb. Direct comparison between the capillary tube and orifice results should not be made since the expansion device change involved some change in refrigerant distribution, and the superheat criteria were different. Also, the two test series were separated by a nine month period during which this heat pump was used for another test series which could have resulted in some wear on the equipment.

The charging criteria for the capillary tube tests was 14°F of superheat leaving the evaporator at the 95°F outdoor ambient cooling test condition. For the orifice tests this was reduced to 10°F. This amount of superheat was desired for this test series for two reasons. First, it was desired to quantify cooling mode performance of the nonazeotropic refrigerant without the composition shift that would occur with flooding into the accumulator. Second, it was desired to use the refrigerant-side mass flow multiplied by the enthalpy change as a secondary capacity measurement method to establish confidence in the tabulated refrigerant mixture properties. This capacity measurement method as specified in ASHRAE Standard 37-78 requires 3°F of subcooling entering and 10°F of superheat leaving the indoor coil to ensure its accuracy. Since these tests were performed, ASHRAE Standard 116-83 has been adopted which allows use of the refrigerant enthalpy flow method with 5°F of superheat leaving the indoor coil.

Table 1. Summarized Results for Cooling Mode Tests Performed with a 65%/35% mixture of R13B1/152a

95°F, DoE "A" Rating Condition

Expansion Device, I.D., In.[b]	Cap	0.0781	0.0807	0.0820	0.0846	0.0846	0.0938	.0938[f]
Air Side Capacity, Btu/hr	27,300	27,320	27,590	27,880	28,130	28,350	27,450	30,490
Latent Capacity, %	15.7	16.3	16.3	17.1	18.8	16.5	15.9	31.9
EER (Total System)	6.26	6.27	6.30	6.45	6.48	6.47	6.34	5.85
Refrigerant Charge, lbs	9.5	9.7	--	9.5	--	--	--	--
Refrigerant Mass Flow Rate, lbs/hr	531	549	571	568	577	608	578[a]	896
Subcooling at Exp. Device, °F	19	6.6	2.0	1.3	1.1	0.5	0	4.4
Superheat Leaving Evaporator, °F	13	11.6	10.1	9.85	10.1	3.4	9.7	13.3
Compressor Suction, psia	82.8	88.7	90.9	90.9	91.2	93.4	91.2	120.9
Compressor Suction, °F	75.5	75.0	73.8	74.2	74.3	66.8	74.2	67.8
Compressor Discharge, psia	317	312	297	297	296	296	294	376
Compressor Discharge, °F	221	212	208	208	208	197	207	204
Compressor Power, W[c]	3960	3857	3882	3830	3845	3884	3836	4715
Fan Power, W[e]	504	500	500	493	495	497	493	496

82°F, DoE "B" Rating Condition

Air Side Capacity, Btu/hr	27,580	28,230	29,060	29,670	29,340	31,600	28,880
Latent Capacity, %	18.5	19.7	18.2	20.3	20.6	20.8	20.2
EER	6.77	7.05	7.17	7.33	7.21	7.57	7.13
Refrigerant Mass Flow Rate, lb/hr	494	513	542	552	567	599	552[a]
Subcooling at Exp. Device, °F	18.3	7.3	3.8	1.2	2.7	1.4	0
Superheat Leaving Evaporator, °F	20.7	18.2	15.1	14.0	13.5	4.0	14.7
Compressor Suction, psia	74.8	80.5	83.4	85.1	83.6	89.9	84.0
Compressor Suction, °F	74.0	73.1	71.2	70.4	71.1	66.2	72.0
Compressor Discharge, psia	271	252	252	252	265	255	249
Compressor Discharge, °F	214	203	198	196	197	187	197
Compressor Power, W[d]	3570	3507	3572	3558	3573	3678	3554
Fan Power, W[c]	504	497	497	491	495	495	497

[a] The mass flow rate for this test in which there was no subcooling was estimated from the refrigerant density entering the compressor.

[b] Cap implies 2 capillary tubes, 0.08" I.D. x 51" long. Otherwise the I.D. for a single 0.5" long orifice is given.

[c] Includes outdoor fan power of approximately 303 W.

[d] Includes outdoor fan power of approximately 309 W.

[e] Includes control circuit power of approximately 40 W.

[f] This one test was performed with an 85.6%/14.4% mixture of R13B1/R152a instead of the 65%/35% mixture used for the other listed tests.

Table 2. Summarized Results for Cooling Mode Tests Performed with R22

Expansion Device, I.D., In.[b]	Cap	Cap	0.0610	0.0670	0.0730	0.0781	0.0846	0.0938
95°F, DoE "A" Rating Condition								
Air Side Capacity, Btu/hr	30,790	32,270	31,710	32,530	31,990	31,630	31,010	30,390
Latent Capacity, %	19.5	22.4	21.8	22.7	23.2	20.9	20.2	20.4
EER (Total System)	7.12	7.42	6.97	7.32	7.30	7.17	7.17	6.94
Refrigerant Charge, lbs.	7.8	---	10.9	9.7	8.9	8.0	8.3	7.2
Refrigerant Mass Flow Rate, lbs/hr	470	483	486	501	501	505[a]	505[a]	505[a]
Subcooling at Exp. Device, °F	13.7	13.9	24.2	18.0	8.7	0	0	0
Superheat Leaving Evaporator, °F	15.6	13.5	10.1	10.0	9.9	9.9	10.1	10.8
Compressor Suction, psia	82.9	84.8	90.4	91.2	90.5	91.1	91.2	91.6
Compressor Suction, °F	75.4	72.6	72.6	71.7	72.4	72.5	73.0	74.6
Compressor Discharge, psia	278	280	299	287	280	279	275	273
Compressor Discharge, °F	232	228	235	226	225	224	224	223
Compressor Power, W[c]	3819	3867	4053	3947	3902	3932	3891	3884
Indoor Fan Power, W[e]	504	484	497	500	479	479	479	495
82°F, DoE "B" Rating Condition								
Air Side Capacity, Btu/hr		33,060	31,320	32,540	32,950	33,550	32,100	31,110
Latent Capacity, %		22.3	23.3	23.5	25.1	23.5	22.1	22.8
EER		8.30	7.71	8.02	8.15	8.23	7.95	7.76
Refrigerant Mass Flow Rate, lbs		449	442	466	480	498	484[a]	473[a]
Subcooling at Exp. Device, °F		16.9	23.1	18.0	11.0	7.2	0	0
Superheat Leaving Evaporator, °F		21.0	19.7	17.4	15.2	13.4	15.0	16.8
Compressor Suction, psia		76.6	80.7	82.7	84.1	86.9	84.9	83.6
Compressor Suction, °F		71.4	71.7	70.2	69.6	68.7	70.3	72.4
Compressor Discharge, psia		236	248	240	235	236	231	229
Compressor Discharge, °F		219	225	216	212	208	209	212
Compressor Power, W[d]		3498	3573	3561	3567	3599	3545	3512
Indoor Fan Power, W[e]		484	491	497	475	479	502	497

[a] The mass flow rate for those tests in which there was no subcooling was estimated from the refrigerant density entering the compressor.

[b] Cap implies 2 capillary tubes, 0.08" I.D. x 51" long. Otherwise the I.D. for a single 0.5" long orifice is given.

[c] Includes outdoor fan power of approximately 303 W.

[d] Includes outdoor fan power of approximately 309 W.

[e] Includes control circuit power of approximately 40 W.

For both binary and conventional refrigerant fixed-area-expansion-device heat pumps, this level of subcooling (3°F to 5°F) is typical, but the level of superheat is high. Typically at the 95°F rating point superheat would be 5° or less. Superheat levels of 5°F to 10°F would be typical of thermostatic expansion valves systems operating at this rating point. Although the design or simulation of an expansion valve system was not included as part of this project, the comparative results are probably quite close to those which would be obtained with a suitable cross-charged expansion valve. It is more likely, however, that an expansion device for a binary refrigerant system would employ an electric valve sensing both outdoor temperature and liquid level in a receiver or accumulator, in addition to temperature and pressure leaving the evaporator.

A value of 0 is listed in Tables 1 and 2 for subcooling at the expansion device when subcooling was lost as indicated by a lack of agreement between the refrigerant and air side capacities.

The binary test shown in column 6 of Table 1 has minimal superheat. This test was conducted since many likely control strategies would result in less superheat than was used for these tests. The binary test shown in column 8 has an increased percentage of R13B1 to show the effect of this variable in the cooling mode.

The expansion device and charge are listed only for the 95°F test. The 82°F test tabulated immediately below each 95°F was performed with the same expansion device and charge on the same or the following day.

The capacity and efficiency test results are also summarized in figure 5. The NBS steady-state heat pump simulation model, HPSIM [8], was used to verify the shape of these curves for the R22 tests and confirmed the observation that as the expansion device becomes overly restrictive the 82°F and 95°F capacity approach each other and eventually cross. The shape of these graphs for the binary refrigerant are quite similar, showing the above described narrowing of the 95°F and 82°F capacity difference for small orifices and showing simultaneous peaks in capacity and efficiency.

The orifice giving the highest capacity at 95°F has a 30% smaller area for the R22 tests and a 6% greater area for the binary tests than the orifice area giving the greatest capacity at 82°F. For general comparison, the optimum expansion device and charge were chosen as those giving the best efficiency at the 82°F rating point. These orifices were the 0.0781 in I.D. for R22 and the 0.0820 in I.D. for the binary mixture. Best performance for both refrigerants was obtained with minimal high-side pressure while still maintaining some subcooling entering the expansion device.

That the percent latent cooling for a given capacity is not strongly affected by the different refrigerants and their associated different temperature patterns through the evaporator is shown in figure 6 derived from Table 1 and 2. This suggests that the decrease in total capacity of the binary mixture, also included a decrease in latent capacity due to an average increase in evaporator temperature. The apparent continuity of this plot for the two refrigerants as shown by the near coincidence of their respective least square linear regression lines indicates that there is no other substantial difference between them.

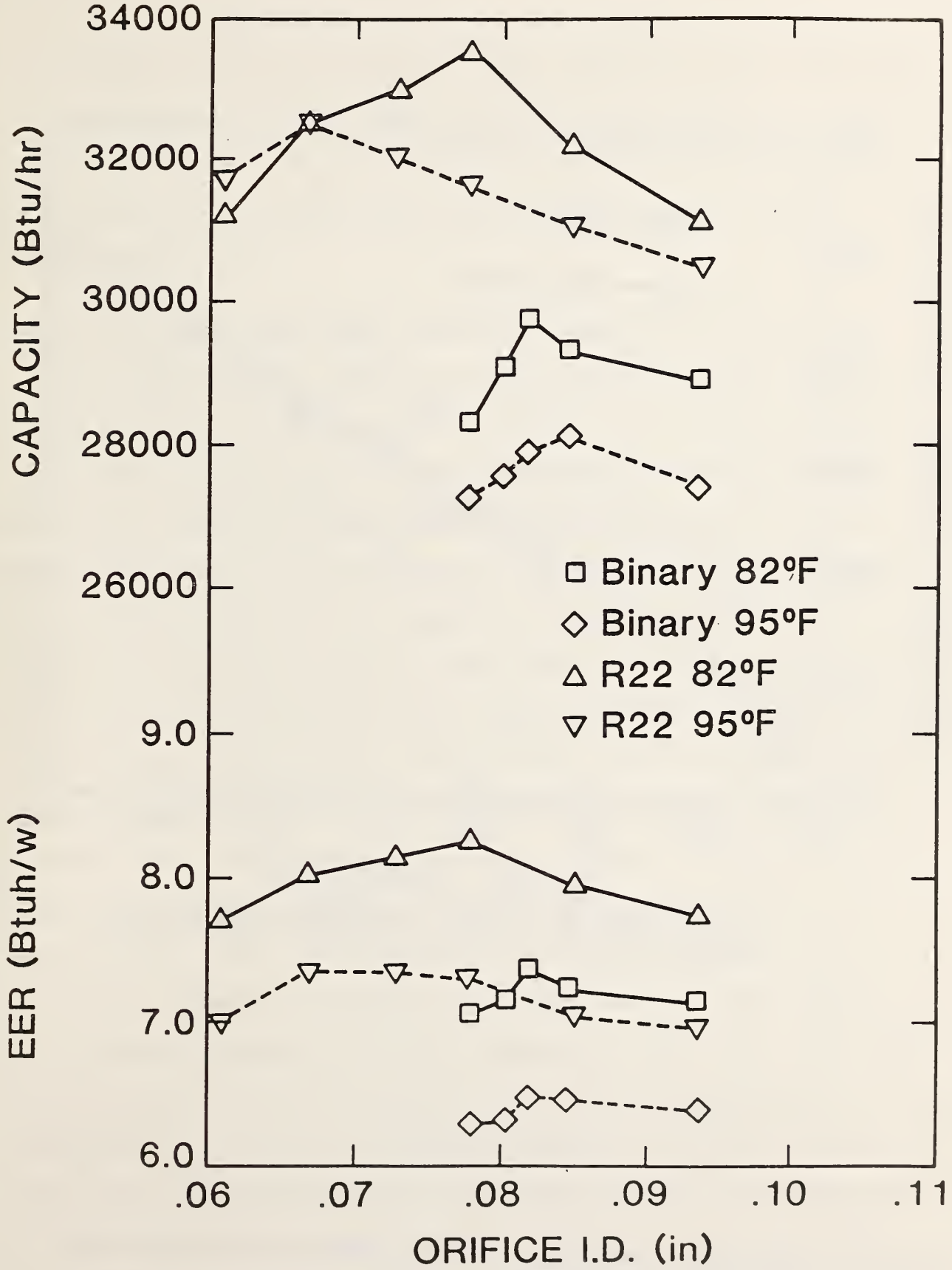

Figure 5. Summarized cooling mode test results.

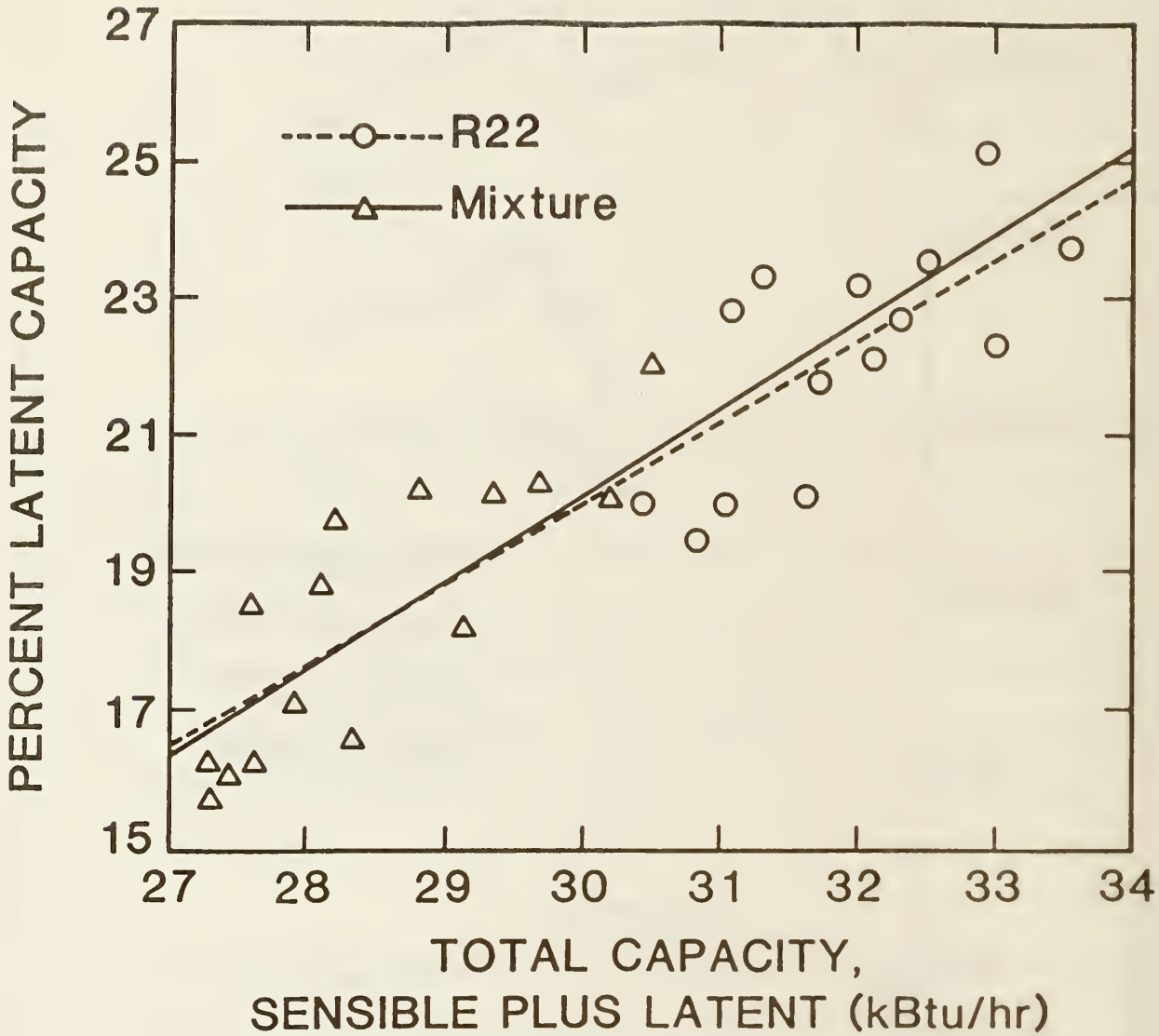

Figure 6. Comparison of latent capacity as a function of total capacity.

For the mixture to have the same percent latent cooling as the R22 case, the air flow rate would have to be reduced approximately by the ratio of their respective capacities. This air flow reduction would result in a lowering of the evaporator saturation temperature and in a small additional loss of capacity and efficiency.

Plots of return bend temperatures through the evaporator for a typical test are shown in figure 7. The saturation, bubble and dew lines shown are calculated from pressures at the evaporator inlet and outlet, assuming a straight line gradient through the coil. The R22 temperatures can be seen to follow the saturation temperature line predicted from these pressures until the refrigerant reaches a quality of unity, after which point it rapidly reaches the imposed conditions of 10°F of superheat. The binary refrigerant temperature gradient results from a tradeoff between the rate of heat gain and pressure drop. The most rapid period of temperature rise occurs when the coil circuitry splits in half, reducing the mass flow in each circuit accordingly, and simultaneously is routed to the front of the coil where the highest heat gain rate occurs. The temperature rise through the binary evaporator, is not as great as the difference between the dew and bubble temperatures at this pressure (18°F) . This is due to the fact that while the changing liquid composition is causing an increase in fluid temperature, the flow pressure drop is causing a decrease in saturation temperature of the fluid. The actual temperature rise through the evaporator for the binary refrigerant was approximately 14°F and that of the R22 approximately 1°F. This is, however, a result of the 10°F superheat criteria reinforcing the temperature gradient for the binary refrigerant and cancelling that of the R22. If the refrigerant left the evaporator as saturated vapor, the temperature difference, inlet-to-outlet, assuming the same pressure drop, for the binary refrigerant would be

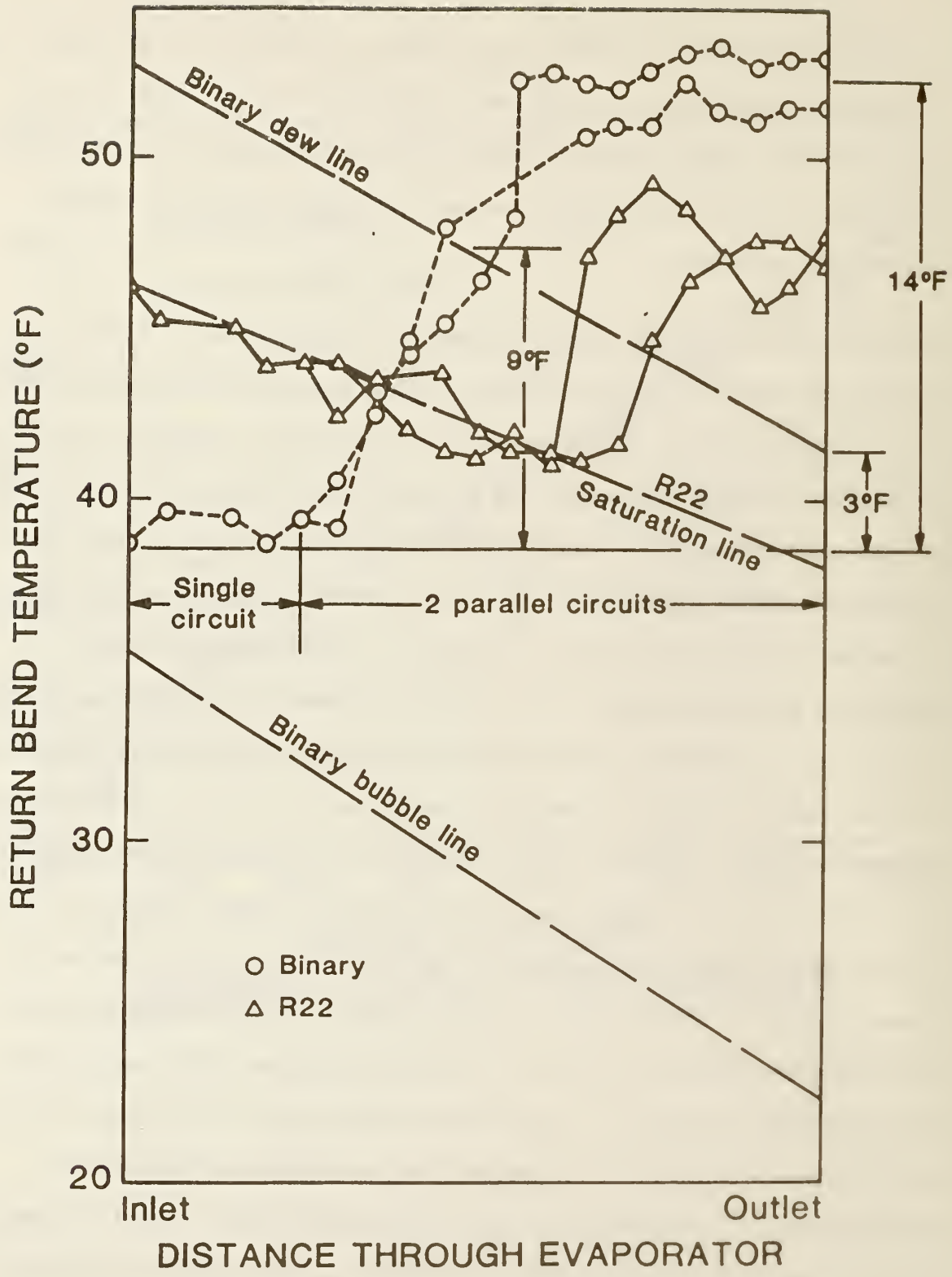

Figure 7. Evaporator (indoor coil) return bend temperatures during a typical 95°F, DoE "A", cooling test.

only 3°F and that of the R22 would be -8°F. The actual temperature gradient for the binary refrigerant while it is in saturation is indicated in figure 7 as 9°F. The temperature difference (gliding temperature effect) of this mixture through the evaporator tends to be of the same order of magnitude as that for R22. In general the value for a binary mixture would be greater or less than that for R22 depending on the temperature difference between its bubble and dew lines, the pressure gradient, and the specified amount of leaving superheat. Return bend temperatures are shown and discussed for both a typical condensing operation and for a flooding evaporator in the following section on heating test results.

The refrigerant charge was not measured for most tests. This was because the unit was charged from separate bottles of the pure components and because as the charge was adjusted to obtain the required superheat and composition frequent addition or removal of small amounts of refrigerant was necessary. This resulted in considerable uncertainty as to the final remaining charge because of the cumulative small errors.

The refrigerant mass flow rates listed for tests in which the liquid refrigerant was subcooled were directly measured with the turbine flow meter. For those tests in which subcooling was lost at the turbine meter, an approximation was made at either test condition "A" or "B" by assuming a constant volumetric flow rate at the compressor suction line and using the measured pressures and temperatures to calculate the refrigerant specific volume.

A principal reason for performing these expansion device optimization tests was the concern about the high pressures observed during the original binary

refrigerant tests which used the capillary tube sized for R22. The improvement in observed pressure at the most severe of the cooling test conditions, 95°F, is summarized in Table 3.

Table 3. Comparison of System Pressures at the DoE 95°F, "A", Test Condition

Refrigerant	R22	R22	Binary	Binary
Expansion Device (cap. tube or orifice diameter, in.)	Cap	.078	Cap	.082
Discharge Pressure, psia	278	279	317	297
Discharge Temperature, °F	232	242	221	208
Suction Pressure, psia	82.9	91.1	82.8	90.9
Pressure Ratio	3.35	3.06	3.83	3.27
Pressure Difference, psi	195	188	234	206

The increased suction pressure for the orifice tests over the capillary tube tests for R22 is a reflection primarily of the change in test plan to a lower value for the refrigerant superheat leaving the evaporator since the expansion device was essentially optimized in both cases. Optimization of the expansion device did reduce the binary pressure ratio to a value between the listed R22 values. The pressure difference remains slightly higher than for R22. Compressor discharge temperature, also listed in Table 3, is seen to be consistently better (i.e., lower) for the binary mixture than for R22.

5. HEATING MODE TESTS

Heating mode test results are summarized in Table 4 for those tests performed with the binary refrigerant mixture and in Table 5 for those tests performed with R22. As indicated in Tables 4 and 5, these tests were performed at both the DoE 47°F and 17°F outdoor ambient test conditions. In both cases, the specified indoor entering air condition was 70°F. The refrigerant charge used for these tests was that which had produced the best efficiency at the 82°F cooling rating condition as shown in Tables 1 and 2. For the binary tests, this resulted in a charge of 9.5 lbs with the 0.0820 in. I.D. orifice installed in the indoor coil for cooling mode operation. For the R22 tests, a charge of 7.17 lbs was used with the 0.0780 in. I.D. orifice installed in the indoor coil for cooling mode operation. Caution should be exercised in making direct comparison between the capillary tube and orifice results since the expansion device change involved changes in distribution and in superheat criteria. Also, these two test series were separated by a nine month period during which this heat pump was used for a different series of tests. This could have resulted in some wear which might bias the results.

The capacity and efficiency results listed in Tables 4 and 5 are summarized in figures 8 and 9. The outstanding observation from these figures is the insensitivity of binary capacity to orifice size. An exception was the smallest orifice at 47°F which presumably failed to flood the evaporator. It appears that the capacity gain from concentration shift is being offset by the capacity loss resulting from the incomplete condensation leaving the condenser. This point is illustrated in figure 10 in which the enthalpy change through the condenser is compared to the value that would have resulted had complete condensation taken place.

Table 4. Summarized Results for Heating Mode Tests Performed with a Mixture of R13B1/R152a Charged to a 65%/35% Original Composition

				47°F DoE Rating Condition						
Expansion Device, I.D., in.,[b]	Cap	0.0650	0.0650	0.0700	0.0730	0.0760	0.0780	0.0807	0.0846	0.0938
Air Side Capacity, Btu/hr	35,660	29,880	31,030	34,460	33,800	35,150	33,870	34,190	34,080	34,160
Charge, lbs	9.5	9.5	9.5	9.5	9.5	9.5	9.5	9.5	9.5	9.5
Operating Composition (%R13B1/%R152a)	65.3/34.7	--	64.6/35.4	--	--	66.7/33.3	--	--	--	--
COP (Total system)	2.71	2.52	2.57	2.76	2.62	2.68	2.61	2.64	2.61	2.58
Refrigerant Mass Flow Rate, lb/hr	454	368	377	489[a]	483[a]	510[a]	496[a]	503[a]	505[a]	527[a]
Quality Leaving Condensor, %, [a]	0	0	0	1.2	0.9	1.0	2.3	2.2	2.5	3.4
Compressor Suction, psia	65.8	59.7	61.2	70.9	70.2	72.5	71.1	71.3	72.1	74.1
Compressor Suction, °F	50	55.6	56.7	38.4	38.1	38.6	37.5	38.0	38.3	38.0
Compressor Discharge, psia	247	215	219	233	231	237	234	233	234	240
Compressor Discharge, °F	192	198	200	176	176	176	175	175	175	173
Compressor Power, W[c]	3378	3008	3054	3320	3308	3372	3339	3336	3360	3421
Indoor Fan Power, W[e]	477	470	479	466	468	470	466	464	468	434
				17°F DoE Rating Condition						
Expansion Device, I.D., in., [b]	Cap	0.0550	0.650		0.0730				0.0846	0.0938
Air Side Capacity, Btu/hr	22,740	20,980	21,050		21,300				20,480	20,510
Operating Composition (%R13B1/%R152a)	72.8/27.2	69.8/30.2	70.8/29.2		73.4/26.6				74.9/25.1	75.9/24.1
COP (Total System)	1.97	1.92	1.92		1.89				1.80	1.77
Refrigerant Mass Flow Rate, lb/hr	347[a]	299[a]	310[a]		335[a]				345[a]	362[a]
Quality Leaving Condensor, %, [a]	2.5	3.1	4.3		8.4				13.1	22.1
Compressor Suction, psia	47.1	46.5	46.9		49.7				50.4	52.7
Compressor Suction, °F	13	14.9	14.6		14.1				13.1	14.0
Compressor Discharge, psia	218	204	204		209				210	212
Compressor Discharge, °F	173	186	186		177				174	172
Compressor Power, W[d]	2903	2716	2732		2819				2849	2912
Indoor fan Power, W[e]	479	479	479		479				479	479

[a] Refrigerant mass flow and quality calculated from air side capacity and volumetric flow meter.

[b] Cap implies a single capillary tube, 0.09 in. I.D. by 37.5 in. long. Otherwise, the I.D. for a single 0.5 in. long orifice is given. In both cases the expansion device directly fed the first pass of the evaporator as indicated in figure 11.

[c] Includes outdoor fan power of approximately 320 W.

[d] Includes outdoor fan power of approximately 340 W.

[e] Includes control circuit power of approximately 40 W.

Table 5. Summarized Results for Heating Mode Tests Performed with R22

	47°F DoE Rating Condition			
Expansion Device, I.D., In., [b]	Cap	0.0630	0.0650	0.0670
Air Side Capacity, Btu/hr	36,200	34,628	35,340	35,220
COP (Total System)	2.79	2.69	2.74	2.73
Refrigerant Mass Flow Rate, lb/hr	383	388[a]	395	398
Quality Leaving Condenser, %	0	1.7	0	0
Compressor Suction, psia	64.7	68.7	68.6	68.8
Compressor Suction, °F	51	31.2	42.0	40.7
Compressor Discharge, psia	222	216	219	218
Compressor Discharge, °F	208	190	196	194
Compressor Power, W [c]	3327	3300	3308	3306
Indoor Fan Power, W [e]	473	473	473	473
	17°F DoE Rating Condition			
Expansion Device, I.D., In., [b]	Cap	0.0630	0.0650	0.0670
Air Side Capacity, Btu/hr	20,510	19,090	20,040	19,740
COP	1.92	1.80	1.89	1.87
Refrigerant Mass Flow Rate, lb/hr	222[a]	205[a]	215[a]	215[a]
Quality Leaving Condenser, %	5.8	6.8	6.7	8.2
Compressor Suction, psia	40.4	43.3	43.5	43.7
Compressor Suction, °F	11	17.4	17.4	17.1
Compressor Discharge, psia	177	175	174	174
Compressor Discharge, °F	203	206	206	205
Compressor Power, W [d]	2642	2621	2627	2610
Indoor Fan Power, W [e]	484	484	484	479

[a] Refrigerant mass flow and quality calculated from air side capacity and volumetric flow meter.

[b] Cap implies a single capillary tube, 0.09 in. I.D. by 37.5 in. long. Otherwise the I.D. for a single 0.5 in. long orifice is given. In both cases the expansion device directly fed the first pass of the evaporator as shown in Figure 11.

[c] Includes outdoor fan power of approximately 320 W.

[d] Includes indoor fan power of approximately 340 W.

[e] Includes control circuit power of approximately 40 W.

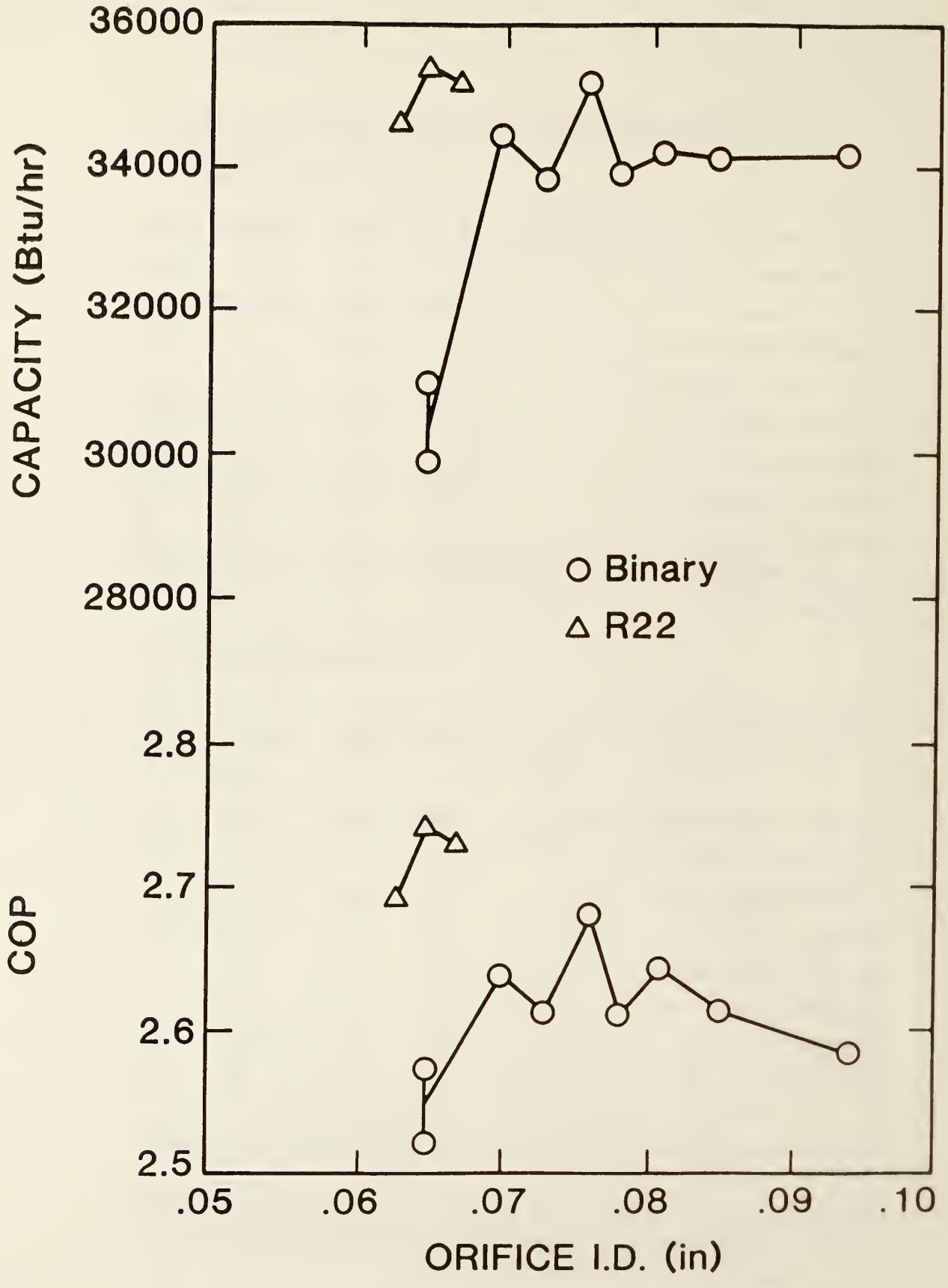

Figure 8. Summarized 47°F heating mode test results.

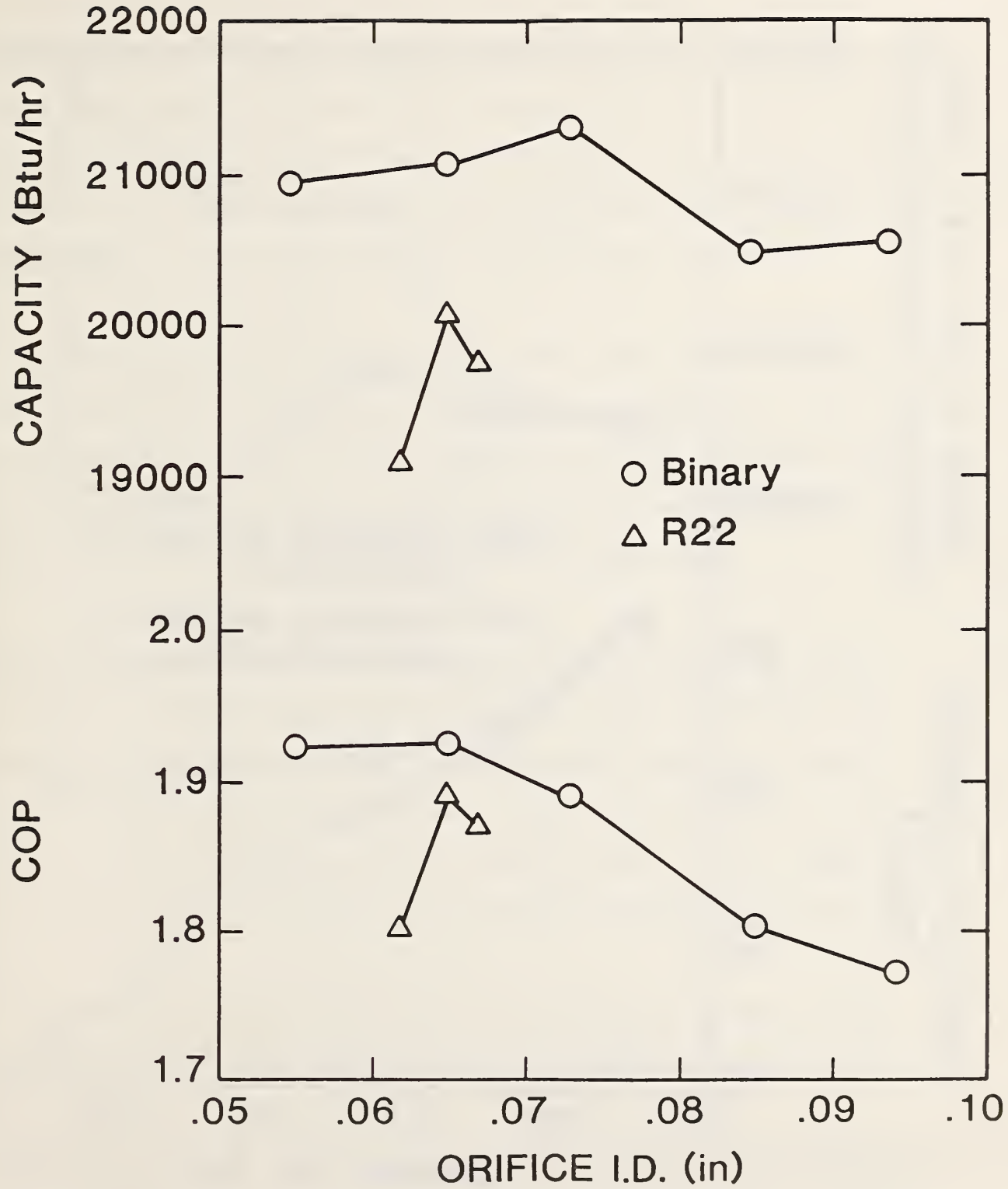

Figure 9. Summarized 17°F heating mode test results.

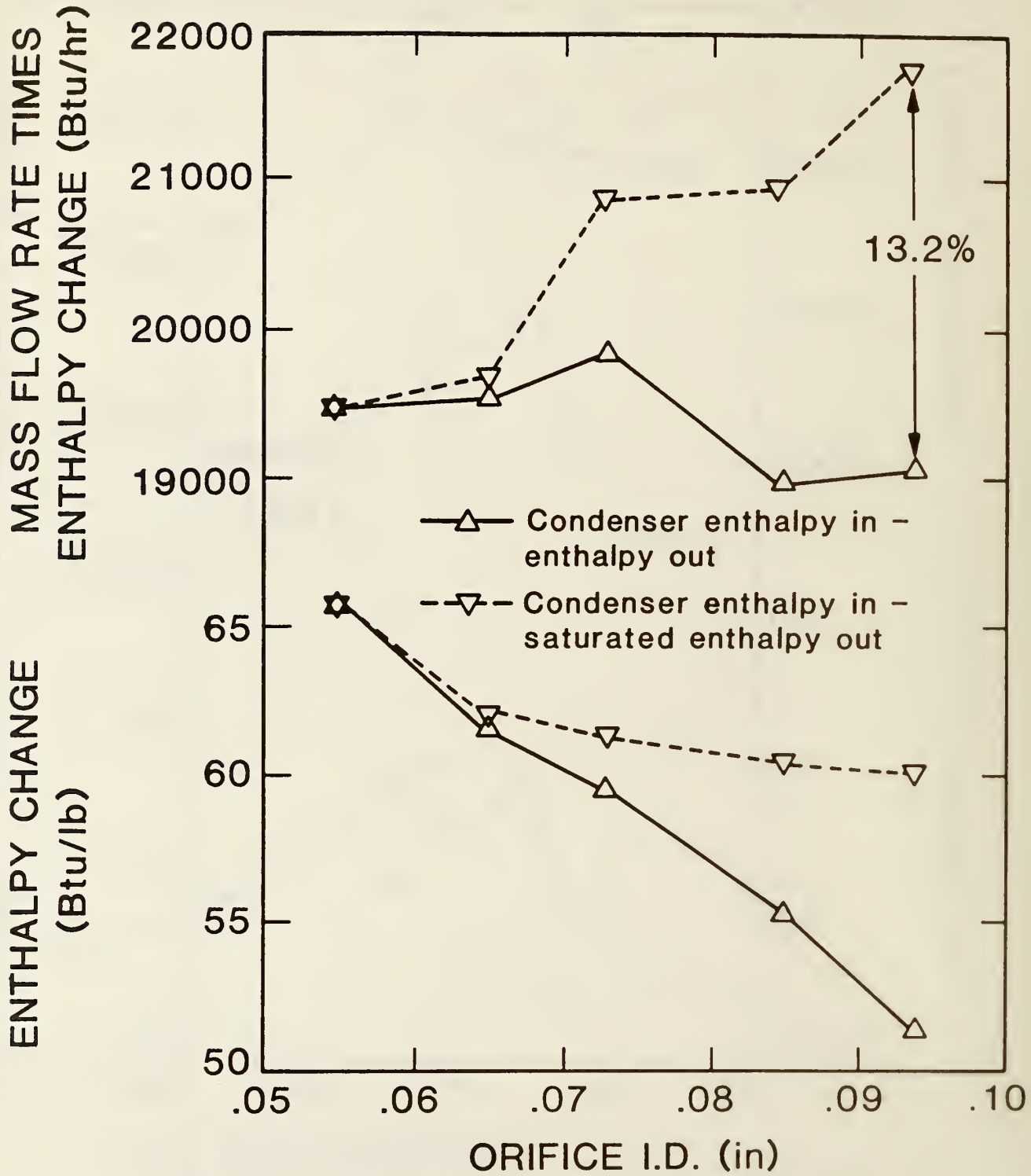

Figure 10. Condenser Enthalpy Change of R13B1/R152a Binary Mixture in Heating Mode at 17°F Outdoor Temperature

The enthalpy used in figure 10 and the tabulated mass flow for most of these tests (as indicated by a superscript in Tables 4 and 5) was calculated by varying the assumed quality at the measured pressure at the turbine flowmeter to find a value which was consistent with the volumetric flow measured by the turbine meter and with the measured air side capacity (see Appendix).

Although the capacity was insensitive to orifice size, the efficiency showed a clear peak for 47°F operation since the shift to concentrations richer in the more dense R13B1, helped to offset capacity loss but not efficiency loss. A similar peak for 17°F operation would be expected if orifices small enough to cause evaporator starving at that temperature had been used.

The binary control strategy, as originally conceived, called for a dry accumulator during 47°F operation and flooding causing composition shift during low temperature operation. It appears that starving the evaporator causes severe efficiency loss and that the best control strategy is to barely flood at 47°F, which still results in composition shift at lower temperatures because the degree of flooding still increases as outdoor temperature drops.

As was observed in the cooling mode tests, the binary discharge pressure is higher and the discharge temperature lower than would be the case for R22.

In figures 11 and 12, return bend temperatures through the evaporator and condenser for R22 and the mixture are compared for 17°F flooded evaporator operation. In this case the refrigerant mixture gives temperatures within the evaporator (figure 11) that rise or fall depending on the relative effects of pressure drop and heat transfer with a leaving temperature approximately 1°F

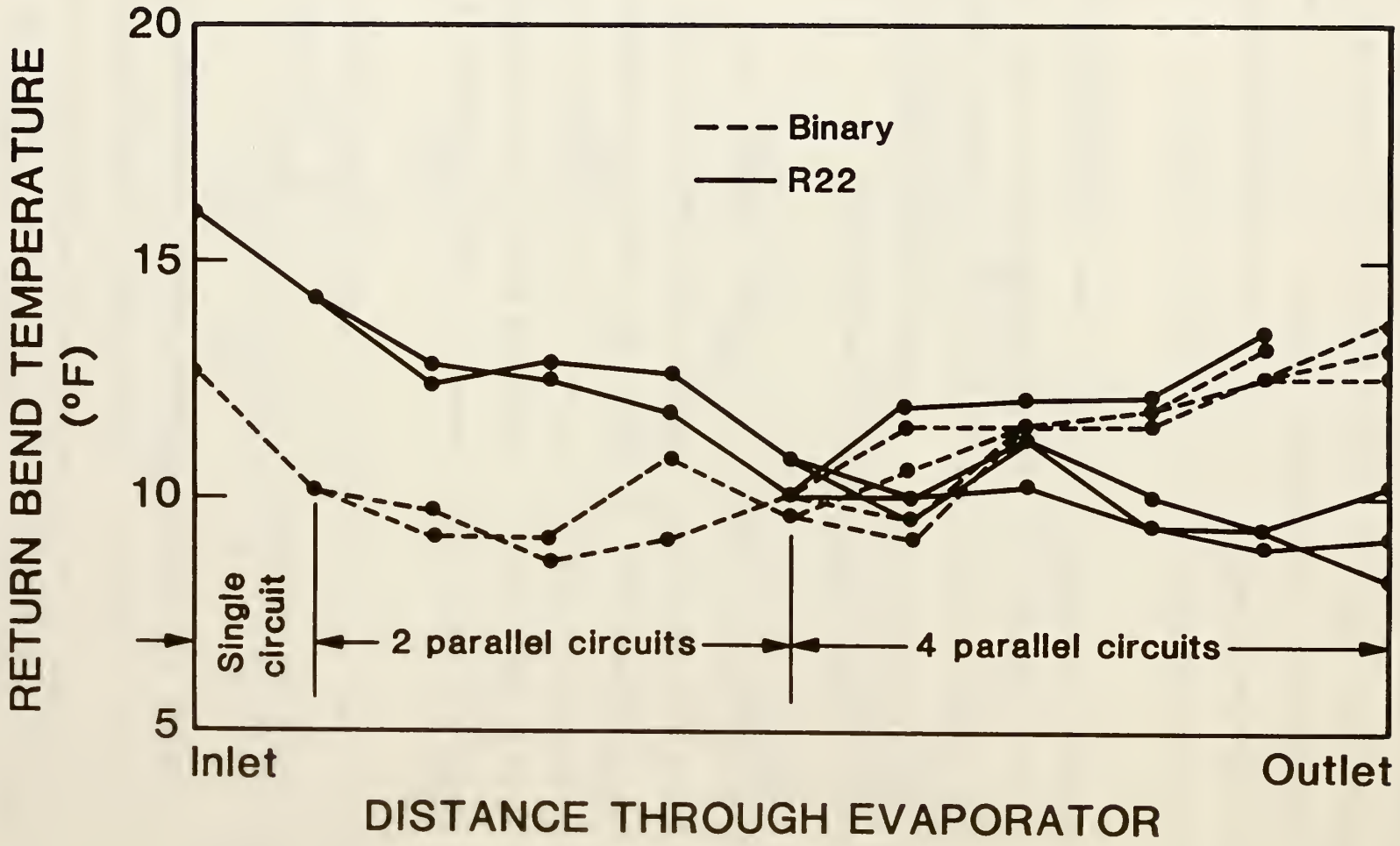

Figure 11. Evaporator (outdoor coil) return bend temperatures during a typical 17°F heating test.

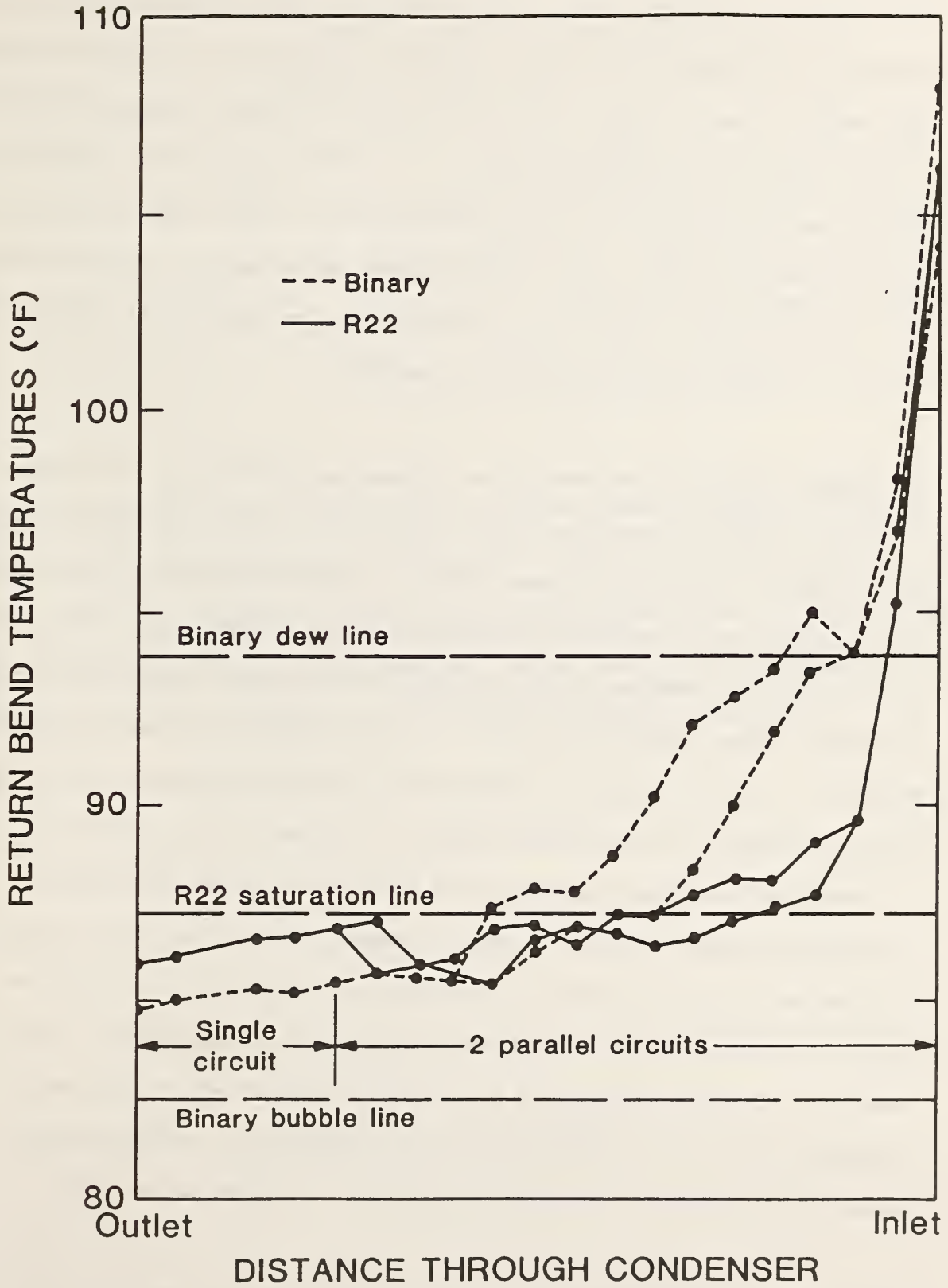

Figure 12. Condenser (indoor coil) return bend temperatures during a typical 17°F heating test.

higher than its entering value, whereas the R22 temperatures steadily fell leaving the evaporator 5°F lower. The heat transfer rate to this coil was more uniform than the indoor coil in that its circuitry zigzagged from front to back instead of proceeding row-by-row. At each branch point the mass flow through each circuit is halved thus resulting in an approximate halving of the flow-pressure-drop rate. Since heat transfer is primarily limited by the air side heat transfer coefficient and surface area, an approximate doubling of the heat transfer rate per pound was observed.

The binary mixture can be seen to go through approximately a 9°F change in the condenser two-phase zone (where the pressure drop and the saturation temperature gradient reinforce) in comparison to an approximately 3°F phase temperature gradient due to pressure drop alone for R22 (figure 12). The pressure gradient was not measurable with the high-side pressure gauges used on the condenser. Hence horizontal bubble, dew, and saturation lines are shown in figure 12. The 3°F saturation temperature difference observed for the R22 would correspond to a saturation pressure difference of approximately 7.5 psi. It should be noted that compared to an evaporator, condenser pressure gradients are less because the lower average void fraction of the condensing refrigerant results in lower velocity and, consequently, lower pressure drop. Also, for this mixture, the difference between the dew and bubble lines is reduced at the high pressure of a condenser in comparison to evaporator pressure levels. For a 65%/35% mixture of R13B1/R152a, this dew-bubble line temperature difference is 14.7°F at 250 psia and 23.5°F at 60 psia.

After it had been observed that the subcooling loss that was occurring concurrently with composition shift was adversely affecting the performance of

the binary mixture, it was decided to perform comparative tests with subcooling at the 17°F heating test condition to evaluate the potential performance obtainable by composition shifting. These tests were performed with an adjustable needle valve in place of the interchangeable orifice expansion devices used for the other reported tests because sufficiently small orifices were not available. The results of these tests are shown in Table 6. A 47°F test with a high concentration of R13B1 is also shown in Table 6 for the purpose of comparison to the data shown in Tables 3 and 4.

The high concentrations of R13B1 shown in Table 6 were obtained by charging the unit with the desired mix of refrigerants rather than as the result of any control strategy affecting a base mixture at 65% R13B1 as was the case in the tests recorded in Table 3. The expansion device was adjusted for best capacity which in all cases was at the point of marginal subcooling.

Table 6. Heating Tests with Subcooling and Manually Adjustable Needle Expansion Valve.

Outdoor Ambient Air Temp., °F	17.4	16.9	46.4
Refrigerant, (R22 or % R13B1)	R22	85.9%	85.7%
Air Side Capacity, Btu/hr	21,500	25,460	39,130
COP (Total System)	1.98	2.00	2.41
Refrigerant Mass Flow Rate, lb/hr	216	483[a]	790[a]
Compressor Suction, psia	42.9	61.6	96.5
Compressor Suction, °F	20	11	33.8
Compressor Discharge, psia	180	259	308
Compressor Discharge, °F	212	178	172
Compressor Power, W	2712[b]	3253[b]	4291[c]
Indoor Fan Power, W	474[d]	473[d]	469[d]

(a) Estimated from compressor suction vapor density.
(b) Includes outdoor fan power of approximately 340W.
(c) Includes outdoor fan power of approximately 320W.
(d) Includes control circuit power of approximately 40W.

It was observed during the low temperature heating tests that large amounts of composition shift could not be obtained without serious loss of subcooling. The simplest solution to this problem and the one tested here is to install a receiver in the liquid line which will remain filled with refrigerant at the circulating composition during both cooling and high temperature heating when subcooling exists in the liquid line. During low temperature operation when subcooling is lost such a receiver would trap bubbles, filling itself with vapor and sending its liquid refrigerant to the accumulator where it would effect a composition shift. This mechanism does require that subcooling be lost, but only by a small amount which should result in a large composition shift. Receiver emptying will not occur completely when subcooling is first lost with the original circulating composition because the composition shift to a greater amount of R13B1 will result in a maintaining of saturation conditions in the accumulator and stable, steady-state operating condition with a partly emptied receiver. This is because the shift to a greater concentration of R13B1 increases vapor density more than liquid density thus increasing compressor capacity relative to expansion device capacity. Liquid level in such a receiver could also be controlled by level sensors operating an electric expansion valve as described by Young [14] instead of the fixed orifice system described in this report.

The actual receiver used in these tests was an inverted oil separator with the oil return line blocked. An inverted oil separator was used instead of a normal receiver so that both inlet and outlet would be on the bottom resulting in insensitivity to direction of flow. The volume was 140 cubic inches which would result in the filled receiver holding approximately 5.8 pounds of either R22 or the 65% R13B1, 35% R152 binary mixture if completely filled. This

extra amount of refrigerant in the receiver during steady-state operations resulted in a total system charge that would have overfilled the accumulator during cyclic operation. Since cyclic testing was not part of this study, no additional system modifications (e.g., larger accumulator or liquid line solenoid) were employed to correct this.

Since a 14 month period had passed since performance of the R22 baseline tests, R22 tests were rerun to reestablish the baseline for comparison to the receiver installed tests. For all tests listed in Table 7, the unit was charged in the cooling mode to 10°F superheat leaving the evaporator at the 95°F test condition. The cooling mode orifice used in charging with R22 was .0780 in I.D. The cooling orifice used for charging for the mixture tests was .0820 in I.D. with the exception of the heating test performed with the .0670 in I.D. orifice. This test was charged at 95°F using a .0807 in I.D. orifice to insure that no flooding was occurring. The charging composition was 65% R13B1/35% R152a. As is shown in Table 7, the performance with R22, particularly at low temperature, had degraded in comparison to the performance listed in Table 5. This is attributed to wear resulting from particularly abusive testing during the 14 month hiatus in the binary refrigerant research program. The most abusive of these tests involved cyclic operation with the accumulator removed which would result in severe oil dilution by refrigerant and consequent cylinder wear. Cylinder wear would be expected to be most damaging to performance at the high compression ratios associated with low temperature heating.

Table 7. Summarized Results for Binsry Mixture Heating Tests with Receiver snd Comparable Tests with R22

47°F of Rating Condition

Expansion Device, I.D., In.	.0650	.0571	.0610	.0635	.0650	.0670	.0700	.0730
Operating Composition, %R13B1 or R22	R22	65.0	65.0	65.8	65.2	67.4	65.6	70.5
Air Side Capacity, Btu/hr	34,240	25,600	27,920	30,820	31,570	34,110	33,950	35,230
COP (Total System)	2.66	2.25	2.37	2.51	2.54	2.58	2.63	2.59
Refrigerant Mass Flow, lb/hr	329[a]	322	353	407	412	489	460	537
Quality Leaving Condenser, %, [a]	1.3	0	0	0	0	0	0	0
Compressor Suction, psia	70.5	54.9	58.8	65.0	66.4	73.3	71.6	77.4
Compressor Suction, °F	41.0	55.5	56.3	54.0	56.3	38.1	50.2	42.7
Compressor Discharge, psia	217	208	214	223	225	237	233	249
Compressor Discharge, °F	194	202	199	190	196		185	179
Compressor Power, W, [b]	3291	2860	2976	3123	3164	3396	3310	3988
Indoor Fan Power, W, [d]	488	478	478	474	478	485	477	478

17°F of Rating Condition

Operating Composition, %R13B1 or R22	R22	74.4	75.7	76.0	75.9	77.5	77.1	76.5
Air Side Capacity, Btu/h	18,910	21,100	21,100	21,020	21,100	21,600	21,060	20,960
COP (Total System)	1.78	1.86	1.86	1.85	1.84	1.82	1.83	1.81
Refrigerant Mass Flow, lb/hr	207[a]	326[a]	358[a]	340[a]	339[a]	374[a]	343[a]	341[a]
Quality Leaving Condenser, %, [a]	7.5	2.4	4.0	6.1	6.0	7.0	6.7	7.7
Compressor Suction, psia	44.1	50.9	52.1	52.6	53.3	55.3		
Compressor Suction, °F	18.9	13.5	13.4	13.4	14.1	13.1	14.1	14.5
Compressor Discharge, psia	173.6	217	219	220		226		
Compressor Discharge, °F	205	179	178	178	180		181	181
Compressor Power, W, [c]	2632	2844	2844	2853	2876	2997	2895	2898
Indoor Fan Power, W, [d]	489	479	480	479	483	489	484	486

[a]Refrigerant mass flow and quality calculsted from sir side capacity and volumetric flow meter.

[b]Includes outdoor fan power of approximately 320W.

[c]Includes outdoor fan power of approximately 340W.

[d]Includes control circuit power of approximately 40W.

At the 47°F operating condition (for the mixture tests), the receiver prevented the unit from losing subcooling (indicated by the refrigerant flowrate being listed as directly measured) by partially emptying into the accumulator so as to enrich the circulating refrigerant with R13B1. The smaller orifices resulted in severe performance loss at this temperature by starving the evaporator. This loss with smaller orifices interferes with the concept of choosing an orifice size such that most composition shift would occur at a typical building balance point.

At 17°F, composition shift greater than that which occurred without the receiver was observed and this resulted in improved capacity in comparison to R22.

6. DISCUSSION

The most highly publicized attribute of nonazeotropic mixtures, that of variable temperature phase change and its associated minimal heat transfer irreversibilities in a counter flow heat exchanger with a sensible heat sink or source, seems to have rather limited application for direct working fluid substitution in R22 air-to-air heat pump hardware. Test results in this study confirmed our model predictions that the saturation temperature decrease due to the refrigerant flow's static pressure decrease virtually offsets the increase in composition shift temperature in the evaporator. Thus, the bulk temperature profile of the mixture in the evaporator is in fact more constant than with R22, which has only the saturation temperature decrease phenomenon occurring. Of course, in the condenser the mixture's composition temperature and saturation temperature shifts are additive and a rather significant refrigerant phase change temperature decrease results. However, current outdoor coil designs are typically single row wraparound resulting in almost pure crossflow heat exchange. Furthermore, the reversing action of the heating/cooling heat pump confounds the design problem of the heat exchangers to be effective with mixtures.

Mixtures should be evaluated on a reliability basis as well as energy performance. For the vapor compression cycle this usually means consideration of the discharge pressure and temperature levels as well as the pressure difference and ratio. For a heat pump, the high-stress condition resulting from high pressures and temperatures will occur during the highest condenser operating conditions, which corresponds to the cooling mode.

Table 3 summarizes some system temperatures and pressures for the cooling mode. The 65%/35% mixture can be seen to produce suction pressures substantially the same as R22. For this mixture the discharge pressure is approximately 18 psia higher than R22 (and consequently the suction to discharge pressure ratios are different). The pressure ratio was, on average, 7 percent higher than R22. The discharge temperature was, on average, 19°F lower than with R22. Thus, when using a superheat leaving the evaporator as a charging criterion, this mixture does not produce pressures significantly higher than R22 and its lower discharge temperatures would likely more than compensate for the slightly higher pressures in affecting system life.

The energy performance of the 65%/35% (R13B1/R152a) mixture, charged in the cooling mode to give a similar superheat as R22, was evaluated. The system operated such that the accumulator was dry throughout the cooling mode which meant no shift in composition was occuring. Cooling efficiency was 10% worse than R22 at the 95°F test condition and 11% worse than R22 at the 82°F test condition.

In the heating mode, it was observed that flooding into the accumulator caused an increase in the mass concentration of R13B1 in the circulating refrigerant of up to 11 percentage points with the largest orifice used. As a part of normal fixed orifice system operation, the subcooling was decreased with each increase in orifice size until completely lost thus offsetting this potential gain in capacity and efficiency at lower temperatures. A possible solution for this loss in subcooling is an additional volume (e.g., a receiver) on the high pressure side which could transfer refrigerant to the accumulator without starving the condenser.

In spite of the above control problem, which reduced the performance of the binary refrigerant below expectations, a substantial improvement in low temperature capacity in comparison to R22 was observed. Without the receiver the binary refrigerant exhibited 6.3% more capacity at the 17°F rating point than R22. With the receiver, the capacity was 14.2% better than R22. In both cases this improvement was the result of composition shift brought about by the normal control by the expansion device (orifice). An additional comparison with slight subcooling leaving the condenser and the binary refrigerant artifically adjusted to give an 86% concentration of R13B1 (in comparison to 73% without the receiver and 76% with it installed) resulted in an 18.4% capacity improvement over R22.

The performance of the mixture (i.e., capacity and COP) is shown in figure 13 relative to R22. All of the tests had an initial charge composition of 65% R13B1/35% R152a, which was the operating composition at 47°F. The composition shifted to 76% R13B1/24% R152a at 17°F. The performance results with the receiver as shown in figure 13 have been increased before plotting by the amount their comparable R22 tests had degraded during the previously mentioned interuption in the test program. This composition shift caused less reduction in low temperature performance than occurred with R22 at low temperatures; that is, as the evaporator temperature is reduced, there is more available mixture capacity relative to R22. The empirical results also show a relative improvement in mixture efficiency performance in comparison to R22.

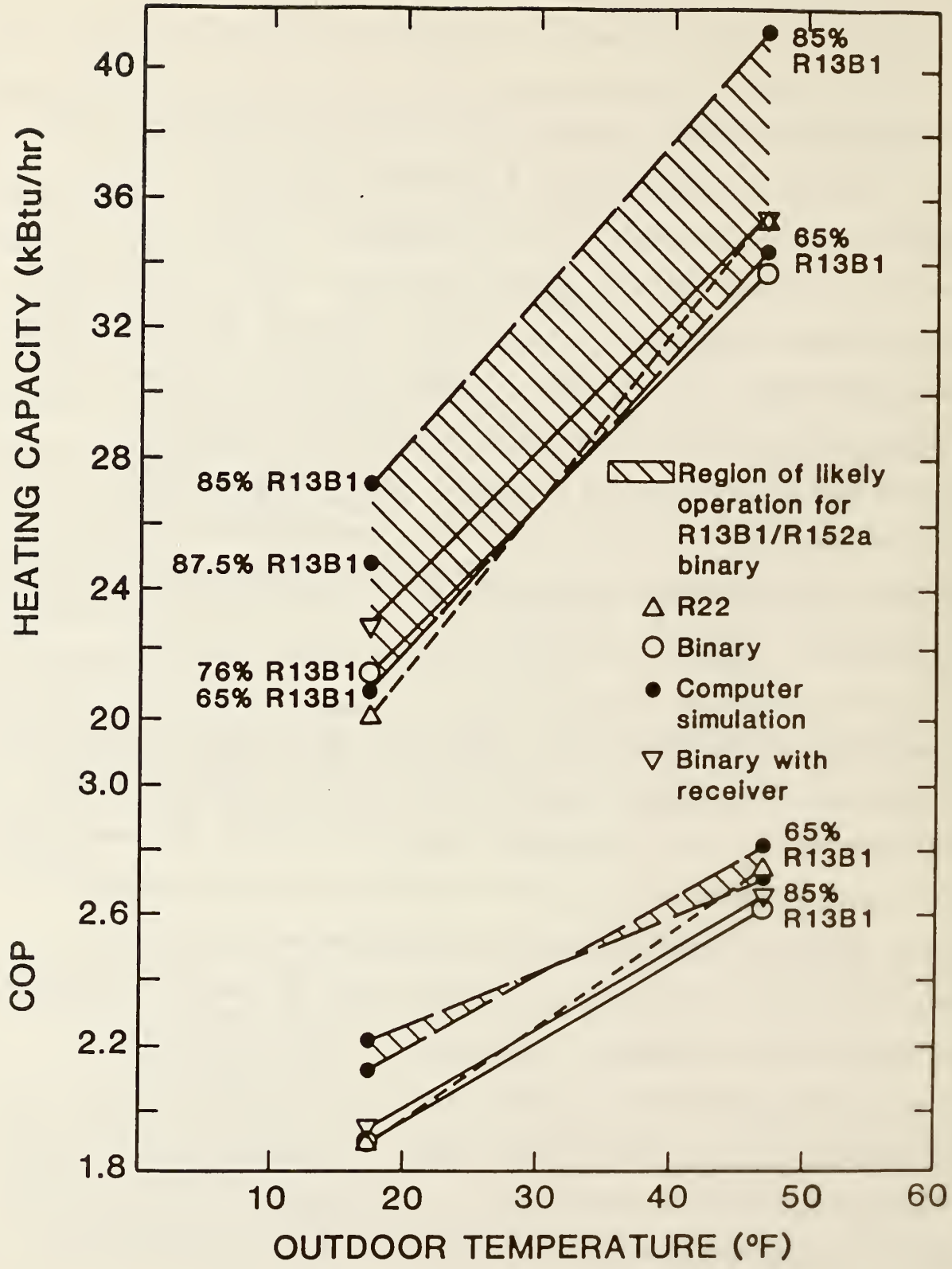

Figure 13. Comparison of binary refrigerant energy performance to R22.

The improvement in comparison to R22 is understandable when the basic properties of the refrigerants are considered. A review of the p-h diagram [11] for the mixture indicates that while the latent heat decreases with increasing percentage of R13B1, the vapor density of the mixture increases enough to more than compensate for this effect due to the higher vapor pressure of R13B1 relative to R152a. Thus, an increase in R13B1 should result in an increase in the product of vapor density times latent enthalpy to which capacity is approximately proportional for a compressor with a constant volumetric flow rate (i.e., positive displacement machines). Also, as the outdoor temperature decreases from 47°F to 17°F, the suction pressure does not have to decrease as much to attain the necessary evaporator temperature because of the composition increase in R13B1. The discharge pressure also increases with shifting composition but at a slower rate than the suction pressure so that the (P_d/P_s) term, of which work is a function, does not increase as much as does capacity when composition shift occurs; thus efficiency also begins to increase relative to the value which would occur without composition shifting.

Also illustrated on figure 13 are the results of the NBS mixtures/heat pump simulation model [12]. The crosshatched band represents the region of likely operation for this mixture. The capacity region is bounded on the bottom by a 65% R13B1/35% R152a circulating composition with a 0°F superheat and a 2°F subcooled condition for both the 47°F and 17°F. The top bound is an 85% R13B1/15% R152a composition with the same operating conditions. These bounds represent the optimum capacity this heat pump could produce with the circulating compositions shown. In order to proceed through this region on any path it is necessary to have full control of the expansion device, the

composition and the charge. For example, the path between the 85% R13B1 point at 47°F and the 87.5% R13B1 point at 17°F represents the fixed orifice and charge case; that is, the current heat pump operation. In this case, these parameters (i.e., expansion device and composition) are not fully controlled resulting in part load performance degraded from the optimum. For this case, there is an associated loss of subcooling when liquid storage occurs in the accumulator, which might well be mitigated with an increase in initial charge.

In summary then, there appears to be an inherent trade-off when operating an unmodified heat pump with R13B1/R152a mixtures so as to increase capacity at lower temperatures. The trade-off is that as the evaporator pressure decreases and begins to flood through to the accumulator and allows the composition shift to occur, the subcooling on the high pressure side also decreases and causes a decrease in the available latent enthalpy difference. A possible solution to this problem might be to increase the amount of initial charge. This would cause an increase in head pressure, which could be a problem in the cooling mode. Another possible solution is to incorporate a receiver in the system in the liquid line between the expansion devices.

The primary areas for future work with binary mixtures are the investigation of additional mixtures, consideration of the changes necessary for conventional heat pumps to take best advantage of the characteristics of mixtures, and, finally, the possibility of more advanced heat pump cycles. Other refrigerant mixtures that have been frequently suggested are R22/R114, R12/R23 and R22/R23. Equipment changes might include water-to-air and water-to-water heat pumps which would allow more ideal counter flow heat exchange. A control scheme monitoring refrigerant level in a receiver as described in [14] may be

useful for air-to-air applications. Since there is interrelation between application, refrigerant properties, and equipment design some parallelism between these different paths should occur. In fact the uncertainties in predicting mixture properties at this time require that, after an initial screening has been made based on predicted properties, final evaluation must be made in a realistically constructed machine operating at conditions of application.

7. CONCLUSIONS

The following conclusions can be drawn from this experimental study:

- Substitution of this particular mixture in an unmodified heat pump, designed for R22 operation, resulted in improved low temperature, 17°F, heating performance (up 6% in capacity, no change in efficiency) at the expense of reduced high temperature heating (down 3% in efficiency) and cooling (down 12% in capacity, 11% in efficiency) performance.

- The low temperature performance was further improved in comparison to R22 by fitting a receiver (up 14% in capacity, 2% in efficiency) at the 17°F rating point.

- The expansion device size should be changed when the refrigerant mixture is changed for one of different properties (liquid vs. vapor density), so as to ensure that proper subcooling will be maintained.

- Efficiency improvement from the gliding temperature effect (Lorenz vs. Carnot cycle) is unlikely in an air-to-air heat pump primarily because of the cross flow design of most current heat exchangers. The gliding temperature effect can be made successful in water-to-water applications.

- Capacity modulation through composition shift is a successful control strategy that will increase seasonal performance in northern applications.

- No potential reliability or safety problems as a result of substitution of the mixture for R22 were observed.

- Future work should be directed toward equipment redesign to better use the characteristics of nonazeotropic mixtures and to analysis of the performance characteristics and potential of other mixtures than the one tested for this report.

8. REFERENCES

1. Cooper, W. D., and Borchardt, H. J., "The Use of Refrigerant Mixtures in Air-to-Air Heat Pumps," XVth International Congress of Refrigeration, Proceedings, Vol. IV, 1979.

2. Cooper, W. D., "The Use of Mixed Refrigerants in Air-to-Air Heat Pumps," ASHRAE Transactions, V. 88, Pt. 1, American Society of Heating, Refrigerating and Air Conditioning Engineers, Inc., Atlanta, Georgia, 1982.

3. Freon Products Division, Freon® 13B1/152a Refrigerant Mixture for Heat Pumps, RT-74, E. I. DuPont de Nemours and Co., Inc., Wilmington, Delaware.

4. Carr, F., "Power Savings in Process Refrigeration," Industrial and Engineering Chemistry, 41, 776-780, 1949.

5. Kazachki, G.S., "Calculation of Two Branch Cycles with Nonazeotropic Refrigerant," Proceedings of Meeting of Commission B1, B2, E1, E2, International Institute of Refrigeration (pp. 153-157), Mons (Belgium), 1980.

6. Schwind, H., "Application of Binary Refrigerant Mixtures and their Presentation in the Enthalpy--Pressure Diagram," Kaltetechnik, 14, 98-105, 1962.

7. "ASHRAE Handbook of Fundamentals", Chapter 16, "Refrigerants," American Society of Heating, Refrigerating and Air Conditioning Engineers, Inc., Atlanta, Georgia, 1985.

8. Domanski, P. and Didion, D., "Computer Modeling of the Vapor Compression Cycle with Constant Flow Area Expansion Device," NBS BSS 155, National Bureau of Standards, Gaithersburg, Maryland, 1983.

9. Parken, W. H., Beausoliel, R. W., and Kelly, G. E., "Factors Affecting the Performance of a Residential Air-to-Air Heat Pump," ASHRAE Transactions, Vol. 83, Part 1, American Society of Heating, Refrigerating and Air Conditioning Engineers, Inc., Atlanta, Georgia, 1977.

10. "Methods of Testing for Rating Unitary Air Conditioning and Heat Pump Equipment, ASHRAE Standard 37-69, American Society of Heating, Refrigerating and Air Conditioning Engineers, Inc., Atlanta, Georgia, 1969.

11. Domanski, P. and Didion, D., "Equation of State Based Thermodynamic Charts for Non-Azeotropic Refrigerant Mixtures," ASHRAE Transactions, V. 91, Pt. 1, American Society of Heating, Refrigerating and Air Conditioning Engineers, Inc., Atlanta, Georgia, (1985).

12. Domanski, P., "Modeling of a Heat Pump Charged with a Non-Azeotropic Mixture Refrigerant," NBS Technical Note 1218, National Bureau of Standards, Gaithersburg, Maryland, 1986.

13. Federal Register, Part III, "Test Procedures for Central Air Conditioners, Including Heat Pumps," Vol. 44, No. 249, p. 76708, December 27, 1979.

14. Young, David J., "Development of a Nothern Climate Residential Air-Source Heat Pump," ASHRAE Transactions, Vol. 86, Part 1, American Society of Heating, Refrigerating, and Air Conditioning Engineers, Inc., Atlanta, Georgia, 1980.

15. Bergles, A.E., Collier, J.G., Delhaye, J.M., Hewitt, G.F., Mayinger, F., "Two-Phase Flow and Heat Transfer in the Power and Process Industries," Hemisphere Publishing Corporation, McGraw-Hill Book Company, 1981.

APPENDIX. OBSERVATIONS ON EXPERIMENTAL TECHNIQUE

This section discusses the experimental techniques that were used for refrigerant sampling for composition analysis, temperature measurement with immersed thermocouples, and two-phase refrigerant mass flow rate estimation.

Two methods of refrigerant sampling were employed, liquid and vapor sampling. Liquid sampling is appropriate for determining the contents of a cylinder or for sampling from a subcooled liquid line of an operating heat pump. Liquid sampling was done with a two chamber bottle consisting of a small chamber to be filled with subcooled liquid and a large chamber separated by a valve to allow expansion of the liquid into room temperature superheated vapor for introduction into a gas chromatograph. This technique requires some knowledge of the mixture composition so that these volumes may be correctly chosen to allow complete expansion into superheated vapor. A pressure gage was found useful to check for superheat after expansion. In some cases, if expansion results in saturation it may be possible to revaporize the sample to a superheated vapor state in a hot water bath and then bleed the sample down to a mass that will result in superheated vapor at room temperature. When connecting the bottle to the sample ports, refrigerant should not be blown to clear the line of air as this will cause composition shift in the line from which the sample is to be drawn. Inclusion of air does not affect the ratio of the two refrigerants as measured by the gas chromatograph.

When taking a vapor sample, vapor from a superheated line in the heat pump was bled into the sample bottle until a pressure was reached that was adequate for injecting the sample into the chromatograph but was well below saturation.

In both sampling techniques, oil should not be allowed to enter the bottle since the different refrigerants will absorb into the oil in proportions different from their circulating composition and will be rapidly released from the oil in the low pressure of the sample bottle. Sampling tees, therefore, should point upward, to avoid trapping oil. If a downward facing fitting must be used for vapor sampling, vapor should be blown shortly before sampling to clear the line.

As was discussed in Section 4, an attempt was made to read refrigerant temperatures with immersed, through-the-wall thermocouples sealed into hypodermic needles with epoxy. Epoxy failures prevented this from being a technique worth recommendation.

For cooling tests, the majority of the data points at each ambient temperature had subcooling and, thus, a valid measurement of refrigerant mass flow rate using the turbine meter. This was used to calculate the ratio of mass flow to vapor density at the compressor inlet which ratio was then used to estimate the mass flow for the remaining points at that same test condition.

The refrigerant mass flow for heating tests in which two-phase flow existed at the flowmeter was calculated by assuming that the flowmeter correctly measured volumetric flow and using the air side capacity to calculate the quality and mass flow. The equation for R22 tests for calculating quality was:

$$\dot{Q}_{AS} = \dot{V}(h_{in} - (xh_v + (1 - x)h_\ell))/(xv_v + (1 - x)v_\ell) + \dot{Q}_F$$

where: $\dot{Q}_{AS}$ = air side capacity, Btu/hr

$\dot{Q}_F$ = fan power, Btu/hr

h_{in} = superheated vapor enthalpy entering condenser, Btu/lb

h_v = saturated vapor enthalpy leaving condenser, Btu/lb

h_ℓ = saturated liquid enthalpy leaving condenser, Btu/lb

v_v = saturated vapor specific volume leaving condenser, cf/lb

v_ℓ = saturated liquid specific volume leaving condenser, cf/lb

$\dot{V}$ = volumetric flowrate, cf/h

x = quality, mass % of vapor

and for calculating mass flow was:

$$\text{Mass flow} = \dot{V}/(xv_v + (1 - x)V_\ell)$$

For the binary tests a similar calculation was performed with the exception that the computerized properties program returned two phase properties giving: $\dot{Q}_{AS} = \dot{V}(h_{in} - h_{2\emptyset})/v_{2\emptyset} + \dot{Q}_F$ and mass flow = $\dot{V}/v_{2\emptyset}$ which were solved by iteration.

The results given by this method were, for all reported tests, within 10% of (and higher than) those given by ignoring the capacity contribution of the refrigerant vapor and calculating the refrigerant mass flow as:

$$\dot{m} = (\dot{Q}_{AS} - \dot{Q}_F)/(h_{in} - h_\ell)$$

A detailed discussion on the use of turbine meters in two phase flow is given in [15].

NBS-114A (REV. 2-8C)

U.S. DEPT. OF COMM. BIBLIOGRAPHIC DATA SHEET (See instructions)	1. PUBLICATION OR REPORT NO. NBSIR-86/3422	2. Performing Organ. Report No.	3. Publication Date JANUARY 1987

4. TITLE AND SUBTITLE

The Performance of a Conventional Residential Sized Heat Pump Operating with a Nonazeotropic Binary Refrigerant Mixture

5. AUTHOR(S)

William Mulroy, and David Didion

6. PERFORMING ORGANIZATION (If joint or other than NBS, see instructions)

NATIONAL BUREAU OF STANDARDS
DEPARTMENT OF COMMERCE
WASHINGTON, D.C. 20234

7. Contract/Grant No.

8. Type of Report & Period Covered

9. SPONSORING ORGANIZATION NAME AND COMPLETE ADDRESS (Street, City, State, ZIP)

Office of Building and Community Systems
U.S. Department of Energy
(via Oak Ridge National Laboratory)
1000 Independence Avenue, SW
Washington, DC 20585

10. SUPPLEMENTARY NOTES

☐ Document describes a computer program; SF-185, FIPS Software Summary, is attached.

11. ABSTRACT (A 200-word or less factual summary of most significant information. If document includes a significant bibliography or literature survey, mention it here)

This report presents laboratory performance measurements of a relatively unmodified residential heat pump designed for R22 when charged with a nonazeotropic, binary mixture of R13B1 and R152a. Results are presented for various sizes of fixed expansion devices. The effect of gliding temperature within the saturation zone was found to be small. This experimental investigation confirmed that flash distillation within the accumulator would improve low temperature heating performance. The measured performance was approximately 11% lower in both efficiency and capacity than R22 for air conditioning. The high temperature heating efficiency was 3% lower than R22. The low temperature heating capacity was 14% higher and efficiency 2% higher than R22. These results show a substantial improvement over R22 for heating applications at the expense of reduced cooling mode performance. Further performance enhancement for this or other mixtures is expected through various system modifications which remain to be studied.

12. KEY WORDS (Six to twelve entries; alphabetical order; capitalize only proper names; and separate key words by semicolons)

air conditioning; heat pumps; nonazeotropic refrigerants; refrigerant mixtures; refrigerants; refrigeration

13. AVAILABILITY

☒ Unlimited

☐ For Official Distribution. Do Not Release to NTIS

☐ Order From Superintendent of Documents, U.S. Government Printing Office, Washington, D.C. 20402.

☒ Order From National Technical Information Service (NTIS), Springfield, VA. 22161

14. NO. OF PRINTED PAGES

67

15. Price

$13.95

USCOMM-DC 6043-P80